Quaternary Science Reviews 334 (2024) 108719

Contents lists available at ScienceDirect

Quaternary Science Reviews

journal homepage: www.elsevier.com/locate/quascirev

Neuroanatomy and palaeoecology of the Early Pleistocene *Dama*-like deer from Pirro Nord (Apulia, Italian Peninsula)

Flavia Strani [a,b,*], Francesca Di Folco [b], Dawid Adam Iurino [c], Marco Cherin [d], Diana Pushkina [e], Lorenzo Rook [f], Raffaele Sardella [b], Beatriz Azanza [a], Daniel DeMiguel [a,g,h]

[a] Departamento de Ciencias de La Tierra, and Instituto Universitario de Investigación en Ciencias Ambientales de Aragón (IUCA), Universidad de Zaragoza, 50009, Zaragoza, Spain
[b] Dipartimento di Scienze Della Terra, Sapienza Università di Roma, 00185, Rome, Italy
[c] Dipartimento di Scienze Della Terra "Ardito Desio", Università Degli Studi di Milano, Via Mangiagalli 34, 20133, Milan, Italy
[d] Dipartimento di Fisica e Geologia, Università degli Studi di Perugia, Via A. Pascoli, 06123, Perugia, Italy
[e] Department of Geosciences and Geography, University of Helsinki, FI-00014, Helsinki, Finland
[f] Dipartimento di Scienze Della Terra, Paleo[Fab]Lab, Università di Firenze, Via La Pira 4, 50121, Florence, Italy
[g] ARAID Foundation, Universidad de Zaragoza, 50009, Zaragoza, Spain
[h] Institut Català de Paleontologia Miquel Crusafont, Universitat Autònoma de Barcelona, 08193, Cerdanyola Del Vallès, Spain

ARTICLE INFO

Handling editor: Donatella Magri

Keywords:
Cervidae
Early pleistocene
Mesowear
Microwear
Palaeoecology
Palaeoneurology
Stable isotopes

ABSTRACT

Medium-sized deer are frequently found in Early Pleistocene fossiliferous deposits of Southern Europe, and hence they represent a reference group for the Villafranchian fauna. Their evolutionary history is still highly debated, as multiple classifications and systematic revisions have been proposed with specimens being ascribed to several genera such as *Pseudodama*, *Metacervoceros*, *Euraxis*, *Praeelaphus*, *Axis*, *Dama*, or *Cervus*. Whereas most studies focus on the taxonomy of the group, a few have addressed how these cervids evolved in relation to the major Early Pleistocene climatic events such as the onset of the Quaternary glaciations. A remarkably rich collection of *Dama*-like deer has been unearthed from the Early Pleistocene site of Pirro Nord (Apricena, south-eastern Italy). Here we analyse palaeoecological and palaeoneurological data of the Pirro Nord sample to investigate both habitat occupation and the evolutionary history of this group during the Early Pleistocene. To do so, we integrate dietary proxies (dental wear patterns and stable isotope signal) with morphological data from a virtual endocast of a well-preserved male specimen, a largely unexplored research path in cervid palaeobiology studies. Moreover, palaeoneurological data may also provide clues to solve the systematic issue of this group. Dental mesowear results point to a long-term mixed diet for the Pirro Nord deer, while a leaning towards a grazing behaviour is suggested by dental microwear patterns. The range of the stable isotope $\delta^{13}C$ ratios suggests that it foraged on abrasive water-stressed C3 vegetation in warm woodland and semi-open habitats. Palaeoneurological data seems to confirm a closer affinity in the endocranial morphology of this taxon to the extant fallow deer *Dama* compared to other Early Pleistocene forms. Our research represents a novel approach to the study of Early Pleistocene fossil deer palaeoecology that can be extended also to other groups to investigate their evolutionary history in relation to climate changes.

1. Introduction

Fossil deer are amongst the best represented taxa in Europe during the Villafranchian (~3.3–1.2 Ma) and Epivillafranchian (~1.2–0.8 Ma) Land Mammal Ages, with several species being recorded throughout these periods. Among them, the so-called *Dama*-like deer – an informal term used to refer to a diverse group of fossil deer species about the same size of the modern fallow deer but displaying unpalmated antlers with three or four tines and a terminal two-pointed fork – which are commonly found in many Early Pleistocene localities representing one of the reference groups for the European biochronology based on large mammals (Gliozzi et al., 1997). Despite their abundance and frequency in the fossil record, the systematics of this group of cervids is highly

* Corresponding author. Departamento de Ciencias de La Tierra, and Instituto Universitario de Investigación en Ciencias Ambientales de Aragón (IUCA), Universidad de Zaragoza, 50009, Zaragoza, Spain.
E-mail address: flavia.strani@unizar.es (F. Strani).

https://doi.org/10.1016/j.quascirev.2024.108719
Received 6 April 2024; Received in revised form 7 May 2024; Accepted 9 May 2024
Available online 21 May 2024

Abbreviations

IGF	Museo di Storia Naturale, Sezione di Geologia e Paleontologia,Università di Firenze (Italy)
DE	Cava Dell'Erba, Department of Earth Sciences, Paleo [Fab]Lab, University of Florence (Italy)
GP	Gargano Pirro, Department of Earth Sciences, Sapienza University of Rome (Italy)
SABAP_UMB	Soprintendenza Archeologia, Belle Arti e Paesaggio dell'Umbria (Italy)
CZUFLD	Czech University of Life Sciences Prague, Faculty of Forestry and Wood Sciences (Czech Republic)
MZVIII	Museum of the Earth, Polish Academy of Sciencs, Warsaw (Poland)
MCN	Mastozoology Sector of the Museu de Ciências Naturais do Rio Grande do Sul (Brasil)

debated (Di Stefano and Petronio, 1998; Azzaroli, 2001). Different classifications have been proposed over the years, with specimens being ascribed to both fossil (*Pseudodama*, *Metacervoceros*, "*Euraxis*", *Praeelaphus*) (Azzaroli, 1992; Di Stefano and Petronio, 1998; Croitor, 2006, 2014, 2018) and extant deer genera (*Rusa*, *Axis*, *Dama, Cervus*) (De Vos and Reumer, 1995; Kahlke, 1997; Pfeiffer, 1999; van der Made, 2001, 2015; van der Made et al., 2017, 2023; Di Stefano and Petronio, 2002; Petronio et al., 2007) and either lumped into a single genus (e.g., *Pseudodama* or *Dama*), or split into different genera based on cranial (especially antler) or postcranial morphology (SI1). Most studies have thus traditionally focused on their taxonomy and systematics, with fewer research aiming at investigating the palaeobiology of these cervids and their evolution in relation to the Early Pleistocene major environmental and climatic changes following the onset of the Quaternary glaciations.

The Early Pleistocene locality of Pirro Nord (Apricena, south-eastern Italian Peninsula) is renowned for its rich collection of vertebrates and for being one of the few European sites with archaeological evidence of the first fossil human populations that settled in the continent (Berruti and Arzarello, 2016). Strict chronological constraints for the site are unfortunately not available. Biochronological inferences based on mammals provide an age range of approximately 1.7 to 1.3 Ma (Arzarello et al., 2012; Pavia et al., 2012; López-García et al., 2015), a recent study by Duval et al. (2024) however suggests a possible younger age of ~0.8 Ma based on a multi-technique dating approach, although fossils and host sediment may not be coeval as fossils may have been reworked into younger deposits. A younger age for the site was also proposed by Muttoni et al. (2010) suggesting that first human colonization events of Southern Europe occurred during the Marine Isotopic Stage (MIS) 22 (~0.87 Ma) (Muttoni et al., 2011). Nevertheless, Pirro Nord is of pivotal importance as (1) it records one of the Pleistocene major climatic phases with the consolidation of the trend towards cooler and more arid environmental conditions following the initiation of the 41-ka periodicity glacial/interglacial cycles (Lisiecki and Raymo, 2005; Hill et al., 2017) and more specifically, (2) it provides a snapshot of Mediterranean vertebrate assemblages and palaeoecosystems around the Early-Middle Pleistocene Transition (Head and Gibbard, 2005). One of the best represented taxa in Pirro Nord is a *Dama*-like cervid of which abundant fossil remains have been recovered during multiple excavation campaigns (Pavia et al., 2012). The sample includes well-preserved cranial and postcranial elements among which two exceptionally preserved crania stand out (Petronio et al., 2013). Through the years the material has been ascribed to several genera and species (see SI1), and a consensus on its systematic position has not been reached yet. Here, we focus on the more complete of the two crania, namely DE 11-1/ind.A (temporarily stored within the collections of the Paleo [Fab]Lab, Earth Sciences Department of the University of Florence), alongside several other dental remains of the same species from Pirro Nord (Florence and Rome collections) to achieve palaeoecological and palaeobiological information.

Herbivore ungulates are highly sensitive to vegetation change related to climatic shifts and by reconstructing their diets it is possible to obtain information on their niche occupation (Fortelius and Solounias, 2000; Solounias and Semprebon, 2002; Strani, 2021). By analysing the dental wear patterns and isotopic signal of the Pirro Nord deer sample it is thus possible to investigate habitat preference and resource exploitation of this extinct herbivore following the gradual cooling process triggered by the onset of the Quaternary glaciations. On the other side, the study of natural or virtual fossil endocasts can provide in-depth palaeobiological and phylogenetical information. However, few studies have focused on endocasts of fossil deer (Aguirre and De Andrés, 1974; Czyzewska, 1982; Fontoura et al., 2020) and only recently this kind of approach has been attempted on a *Dama*-like Villafranchian species, namely *Pseudodama nestii* from Pantalla (Italy; Cherin et al., 2022). The outstanding cranium DE 11-1/ind.A retrieved from Pirro Nord therefore can be a source of novel valuable information needed to disentangle the evolution of this controversial deer group.

In this paper, a combination of dietary and palaeoneurological analysis from the exceptional Pirro Nord *Dama*-like deer sample associated with comparisons with extinct and extant cervids, is carried out for the first time. Obtained results from this novel approach can provide information on the affinities in terms of neuroanatomy and ecological adaptations between some *Dama*-like deer taxa and modern genera this group has been ascribed to.

1.1. Geological setting

Pirro Nord is a complex of fossiliferous karst fissure fillings located in the municipality of Apricena (southern Italy; Fig. 1A), in the limestone (Upper Mesozoic "Limestone of Bari" formation) quarry district of Cava di Pirro or Cava Dell'Erba on the north-western edge of the Gargano promontory, which is a part of the Apricena-Lesina-Poggio Imperiale mining complex (Pavia et al., 2012). The occurrence of fossil vertebrates

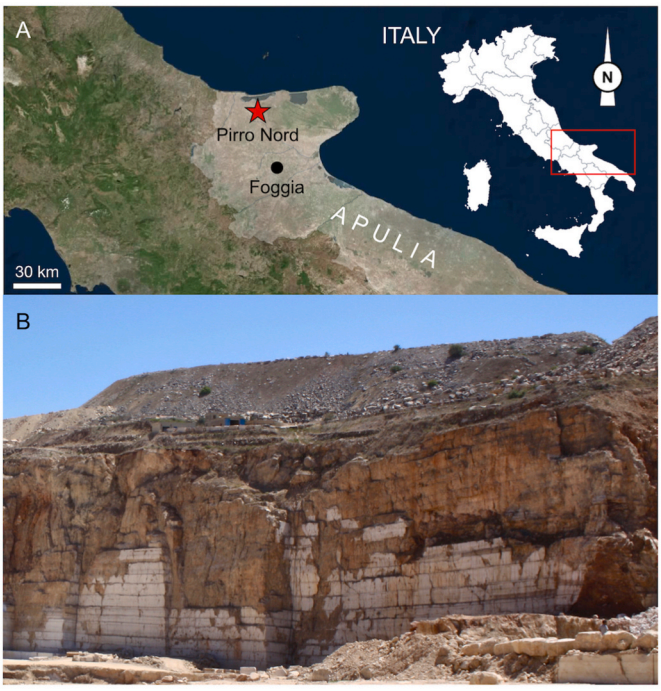

Fig. 1. Geographical location of the Pirro Nord site (A) and picture of one of the fossiliferous outcrops (B).

in the area was reported at the beginning of the 1970s (Freudenthal, 1971) during an expedition of the Naturalis Museum of Leiden (now Naturalis Biodiversity Center). During the following decades systematic field research by several universities (Florence, Sapienza of Rome, Turin, Ferrara) generated a varied collection of Neogene and Quaternary vertebrate remains. The fossiliferous deposits of the site consist of the detrital-clayey fillings of the karst fissure network developed during the Early Pleistocene within the Upper Mesozoic limestone and the overlying Pliocene carbonate succession (Abbazzi et al., 1996), formed alongside the Apricena fault (Zunino et al., 2012) (Fig. 1B).

The palaeontological material described herein is part of the very rich Pirro Nord assemblage, which is composed by more than 100 vertebrate taxa (mammals, birds, reptiles, amphibians, and rare fishes) dated to the late Early Pleistocene (Late Villafranchian; ~1.7–1.3 Ma) according to biochronological analysis (Maul et al., 1998; Berruti and Arzarello, 2016), although a possible younger age of ~0.8 Ma has been recently suggested based on multi-proxy analysis of sediment samples (Duval et al., 2024). Mode 1 stone tools were found in association with the vertebrate remains, representing one of the earliest pieces of evidence of hominin occurrence in the European continent (Arzarello et al., 2007, 2016; Berruti and Arzarello, 2016; Sardella et al., 2018).

2. Material and methods

The abundant *Dama*-like material from Pirro Nord is reported by Petronio et al. (2013), who refer it to *Axis eurygonos*, although De Giuli et al. (1987) had already identified it as "*Dama*" cf. *Nestii*. The cranium DE 11-1/ind.A is figured (with only the basal part of the right antler visible) by Petronio et al. (2013: Text-Fig. 2) but only summarily described as bearing a relatively long splanchnocranium and "rather primitive" teeth. In the same paper, an overall description of the antler morphology is also provided and the cranium is attributed to a sub-adult individual. Some additional cranial features alongside a drawing of the specimen and some measurements are provided by Croitor (2014: 142-144) and Croitor (2018: 111-112), according to which and to the missing middle (trez) tine of the antlers, the Pirro Nord deer should be referred to *Dama vallonnetensis*, as well as those from other European localities such as Le Vallonnet (France; de Lumley et al., 1988), Capena (Italy; Petronio, 1979), Untermassfeld (Germany; Kahlke, 1997; 2001; Breda et al., 2020), and Etulia (Moldova; Alekseeva, 1977). However, according to Azzaroli (1992), Breda and Lister (2013), and Cherin et al. (2022), among others, based on their overall similarity, all Villafranchian (~3.3–1.2 Ma) and Epivillafranchian (~1.2–0.8 Ma) European *Dama*-like deer species with unpalmated antlers should be accommodated into a single, perhaps paraphyletic genus, *Pseudodama*. Given the lack of consensus on how to taxonomically identify the material from Pirro Nord and because our work does not aim to solve the systematics of this taxon and of related ones, we generically refer the studied sample to as "*Dama*-like deer" herein.

The cranium DE 11-1/ind.A was scanned for palaeoneurological analysis (see below). For the dental wear analyses, we used teeth stored at the Departments of Earth Sciences of the University of Florence and of Sapienza University of Rome, selecting the most suitable specimens based on conservation status and age of the individual. Deeply altered teeth (e.g., displaying taphonomic alterations or badly preserved enamel bands) and teeth belonging to either juvenile or old individuals were excluded from these analyses following standard protocols (King et al., 1999; Fortelius and Solounias, 2000).

Comparative data on other *Dama*-like deer samples from the following Italian and Iberian Villafranchian and Epivillafranchian localities were considered: Coste San Giacomo (~2.1 Ma; Bellucci et al., 2014; Strani et al., 2015), Pantalla (~2.2 Ma; Cherin et al., 2022; Cherin et al., 2023), Olivola (~2.0–1.8 Ma; Strani et al., 2018a), Vallparadís Estació (layers EVT7 and EVT12 dated at 0.858 and ~1 Ma, respectively) (Strani et al., 2019).

2.1. Dental mesowear analysis

Mesowear is considered a good dietary indicator in herbivore species, as it represents the cumulative effects of consumed items (both foods and exogenous particles such as dust and grit) on the dental morphology that are produced over months and years (Fortelius and Solounias, 2000; Ackermans, 2020). Traditional mesowear analysis (Fortelius and Solounias, 2000) is based on the sharpness (i.e., morphology) of the cusps and the height of the occlusal relief of the paracone and metacone of upper second molars. This analysis has later been extended to other tooth positions (Kaiser and Solounias, 2003; DeMiguel et al., 2012). In this study occlusal relief (high or low) and cusp shape (sharp, rounded, or blunt) of the apex of the paracone and metacone of upper molars (M1-M3) and the metaconid and entoconid of lower molars (m1-m3) were examined, but if available, M2 and m2 were preferably selected. A mesowear score (MWS) was also calculated based on the combination of cusp shape and occlusal relief (as in Mihlbachler and Solounias, 2006; Rivals et al., 2007; Strani et al., 2019): a score of 0 is given to teeth showing a combination of high relief and sharp cusps; 1 to the teeth with high relief and rounded cusps; 2 to teeth with low relief and rounded cusps; 2.5 to teeth with low relief and sharp cusps; and 3 to teeth with low relief and blunt cusps. A total of 39 specimens were analysed using this method. The obtained data were compared with those of extant ungulates with known diets from Fortelius and

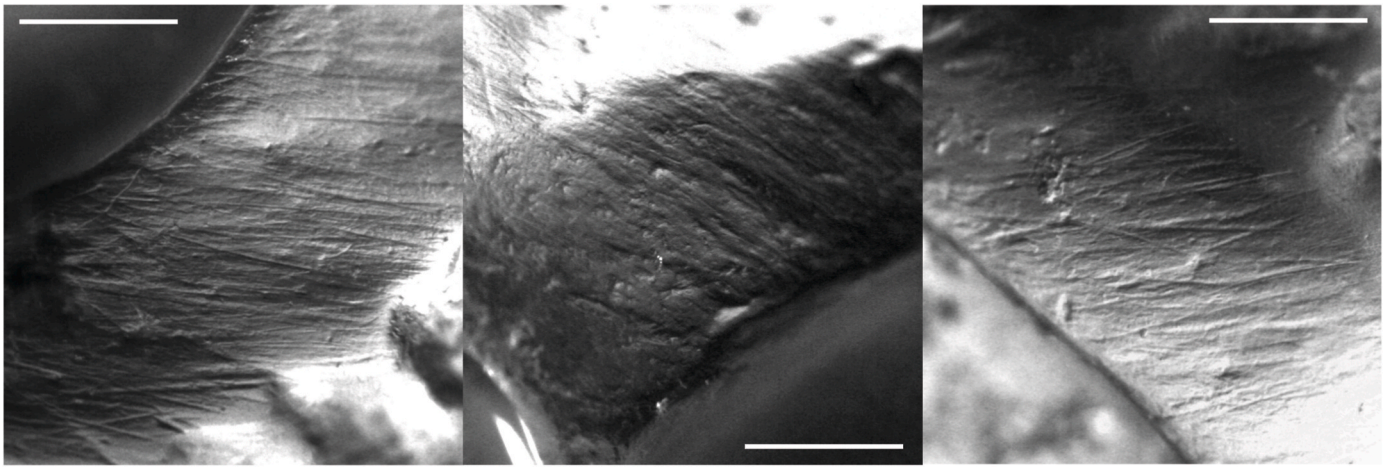

Fig. 2. Photomicrographs of enamel surfaces at 35× magnification of selected teeth of Pirro Nord Dama-like deer. From left to right: right m2 (DE 11-1/9-2); right M2 (DE 60), right M2 (DE 11-1/ind.A). Scale bar: 500 μm.

Solounias (2000) and with *Dama*-like deer from other Iberian (Vallparadís Estació layers EVT7 and EVT12) and Italian (Coste San Giacomo, Olivola) (Strani et al., 2015, 2018a, 2019). Raw mesowear data are available in SI2.

2.2. Dental microwear analysis

Dental microwear represents the abrasion of teeth produced by food and other items consumed during the last few days prior to the death of an animal known as the "Last Supper Effect" (Grine, 1986). Average number of scratches and average number of pits can be used to discriminate between browsers (animals feeding on soft or ligneous plant parts such as twigs, leaves, and fruits), grazers (animals feeding on grass), and mixed feeders (animals which feed on both types of foods) (Solounias and Semprebon, 2002). The percentage of individuals with scratch numbers falling in a low scratch range (0–17%) defined in the 0.16 mm^2 area (as described in Semprebon and Rivals, 2007) can also separate mixed feeders by browsers and grazers. For extant ungulates, the percentages of individuals in the low scratch range are as follows: grazers have 0.0–22.2% of individuals with scratches between 0 and 17; mixed feeders have 20.9–70.0% of individuals with scratches between 0 and 17; and leaf-dominated browsers have 72.7–100.0% of individuals with scratches between 0 and 17 (Semprebon and Rivals, 2007).

Microwear features of dental enamel were examined using a stereomicroscope on high-resolution epoxy casts of teeth following the protocol developed by Solounias and Semprebon (2002). The occlusal surface of the upper or lower molars was cleaned using acetone and then alcohol. The surface was molded using high-resolution silicone (vinylpolysiloxane) and casts were created using clear epoxy resin. The M2 mesial lingual blade of the paracone and the m2 distal buccal blade of the protoconid were preferably selected as areas of study, as these facets are in occlusion during the mastication and on second molars an intermediate wear stage between first and third molars can be observed (Gordon, 1982). If these facets were absent or badly preserved, other facets were sampled. Casts were observed under incident light with a Leica M205 C stereomicroscope at 35× magnification, using the refractive properties of the transparent cast to reveal microfeatures on the enamel (Fig. 2). Microwear features were classified following Solounias and Semprebon (2002), quantifying all categories in a standard square area of 0.16 mm^2. The analysis was carried out using MicroWeaR (Strani et al., 2018b), which classifies features in a semi-automatic way dividing them into four categories: small and large pits (microscopic features with regular, circular, or semi-circular edges), fine and coarse scratches (microscopic finely or coarsely textured striations). The presence of cross scratches (scratches which are oriented perpendicularly to the majority of scratches) and gouges (microwear features similar to pits but larger, deeper and with irregular edges) was also reported. This analysis was carried out by a single person (FDF) to avoid inter-observer errors as recommended by Mihlbachler et al. (2012), who however also points out that true observer blindness can probably be ensured only by using shared microwear image libraries.

Scratch textures were converted into a Scratch Width Score (SWS) to simplify representation of the data by giving a score of '0' to teeth with predominantly fine scratches per tooth surface, '1' to those with a mixture of fine and coarse types of textures, and '2' to those with predominantly coarse scratches. Individual scores for a sample were then averaged to get the SWS value. Coarse scratches are mostly observed in modern C4 grazers, bark eaters, and fruit browsers (Solounias and Semprebon, 2002).

The obtained data were compared with those of extant ungulates with known diets from Solounias and Semprebon (2002) and with *Dama*-like deer from other Vallparadís Estació (layers EVT7 and EVT12) (Strani et al., 2019). Raw microwear data are available in SI2.

2.3. Stable isotope analysis

The stable carbon isotope ratio ($\delta^{13}C$) in tooth enamel bioapatite reflects the presence of C3 and C4 vegetation in lower and mid-latitude habitats as well as a degree of canopy closure versus openness in wooded high-latitude habitats (Vogel et al., 1978; Alcocks, 1988; O'Leary, 1988). Modern C3 plants, including trees, shrubs, and cool-growing grasses, have $\delta^{13}C$ values ranging between −34‰ and −20‰ with a suggested mean of −27‰, in contrast to C4 plants, represented primarily by tropical grasses and shrubs, which have a mean $\delta^{13}C$ values of −13‰ (Bender, 1971; Smith and Epstein, 1971; O'Leary, 1988; Kohn and Cerling, 2002).

The $\delta^{13}C$ values of the carbonate fraction of bioapatite in large mammalian herbivores are enriched by 14‰ in comparison to the plants consumed (diet/ecosystem), expressed by the formula: $\delta^{13}C_{\text{bioapatite}} = \delta^{13}C_{\text{diet}} + 14‰$ (Cerling and Harris, 1999; Kohn and Cerling, 2002). Consequently, $\delta^{13}C$ values with the mean of −13‰ in herbivore enamel indicate wooded environments, $\delta^{13}C$ values lower than −13‰ indicate woodlands and denser forests, whereas $\delta^{13}C$ values higher than −13‰ indicate more open habitats, such as grasslands and steppes in warm temperate and cold boreal environments, in which the plants have $\delta^{13}C$ values higher than - 27‰ (Bocherens, 2014).

The stable oxygen isotope ratio ($\delta^{18}O$) in enamel apatite reflects the source of water consumed, ingested either from drinking from a water source or from food and plants (Bryant and Froelich, 1995). The $\delta^{18}O$ values depict variations in meteoric water due to the source of precipitation and the effects of latitude, altitude, continentality, temperature and evaporation (Dansgaard, 1964; Longinelli, 1984). Crudely, herbivores feeding in open steppe habitat with C4 vegetation and non-obligate drinkers, obtaining water from tree leaves, demonstrate higher or more enriched $\delta^{18}O$ values than the species from forested cooler and more humid habitat (Dansgaard, 1964; Bocherens et al., 1996). Higher $\delta^{18}O$ values are also associated with hotter climate and marine habitats.

The $\delta^{13}C$ and $\delta^{18}O$ ratios were obtained from enamel carbonate fraction of the three right upper molars of adult individuals. The upper enamel layer was cleaned from surface contamination by a diamond-impregnated dremel© borer, after which the enamel powder samples of 16–18 mg were drilled. The samples were pre-treated following the method described by Bocherens et al. (1996), using the Continuous Flow (CF) for collecting carbon dioxide (Bocherens et al., 2009) at the Lab of Stable Isotopes of the Istituto di Geologia Ambientale e Geoingegneria, CNR. Approximately 1.5–2 mg of enamel powder was measured in duplicate/triplicate along with three in-house laboratory standards (MC-200 – Carrara Marble, $CaCO_3$—Merck CCM, and Solnhofen limestone—SLNF, calibrated against international standards NBS18 and NBS19) to normalize the raw $\delta^{18}O_{Ca}$ and $\delta^{13}C_{Ca}$ values to the V-PDB scale. Repeated analyses of internal carbonate standards ($n > 30$) yield 1std dev <0.1‰ for both $\delta^{13}C_{Ca}$ and $\delta^{18}O_{Ca}$. An aliquot of the enamel powder for each sample was weighed and placed into empty vials and analysed by a Thermo Scientific™ Gas Bench II connected to a Thermo Delta Plus isotope ratio mass spectrometer. The data obtained were normalized by a linear calibration equation derived from a plot of accepted versus measured values for the three aforementioned internal standards.

Stable isotopic results are expressed as the following standard δ−notation: $\delta EX = [(R_{sample}/R_{standard}) - 1] \times 1000$, where EX is $\delta^{13}C$ or $\delta^{18}O$ and R is $^{13}C/^{12}C$ or $^{18}O/^{16}O$, respectively. The standards are the marine carbonate VPDB (Vienna PeeDee Belemnite) for carbon and oxygen, and VSMOW (Vienna Standard Mean Ocean Water) for oxygen [NBS18 ($\delta^{13}C = -5.00‰$, $\delta^{18}O = -22.96‰$, relative to VPDB); NBS19 ($\delta^{13}C = 1.95‰$, $\delta^{18}O = -2.20‰$, relative to VPDB)].

We also calculated an approximate percentage of C4 plants in the diet of the analysed specimens, based on the formula: $C4_{\text{food}}\% = (\delta^{13}C_{\text{bioapatite}} - \delta^{13}C_{\text{pure C3 feeder}}) - (\delta^{13}C_{\text{pure C4 feeder}} - \delta^{13}C_{\text{pure C3 feeder}})$, using the enamel $\delta^{13}C$ values for pure C3 and C4 feeders as −12.4‰ and

+1.6‰, respectively (Koch et al., 1998). We calculated temperature (°C) using the formula by Skrzypek et al. (2011), which best described the current relationship between air and water: $T_{air} = 1.804\ \delta^{18}O_W + 26.02$. To convert oxygen carbonate into phosphate values we used the formula: $\delta^{18}O_C = 1.035\delta^{18}O_P + 8.33$ (Lecuyer et al., 2010). The estimates of the $\delta^{18}O$ values of drinking water consumed by species were calculated using the following equation for deer species: $\delta^{18}O_P = 1.13\delta^{18}O_W + 25.5$ (D'Angela and Longinelli, 1990).

2.4. CT analysis

CT images of the DE 11-1/ind.A cranium (slice number: 199) were taken using a Siemens Sensation 64-slice scanner with slice thickness of 1.5 mm and interslice thickness of 0.6 mm. Those of *P. nestii* from Pantalla SABAP_UMB 337643 (slice number: 809) and SABAP_UMB 337655 (slice number: 647) were taken using a Fujfilm FTC Speedia 16-slice scanner with slice thickness of 0.8 mm and interslice thickness of 0.4 mm (Cherin et al., 2022). Those of the extant *Dama* (CZUFLD FaD001, CZUFLD FaD002, CZUFLD FaD003; slice numbers: 913, 845, 566, respectively) and *Cervus elaphus* (CZUFLD ReD001, CZUFLD ReD002, CZUFLD ReD003; slice numbers: 1271, 1513, 719, respectively) were taken using a Siemens Somatom Scope Powerscanner, a multi-detector CT scanner with 16 slices with both the minimal slice thickness and voxel size equal to 0.6 mm (Cherin et al., 2022). For this study, the slice thickness was set to 1.0 mm and the recon increment to 0.5 mm. Finally, the CT images of the extant *Axis* MCN 3310 (slice number: 406) were taken using a Philips Brilliance 16-slice scanner with slice thickness of 0.63 mm and pixel size of 0.30 mm (Fontoura et al., 2020). The segmentation process of the CT images was carried out with Mimics Innovation Suite 21.0, allowing the virtual extraction of the brain endocasts from the crania and the acquisition of their biometric and morphological data. The final editing of the 3D images (e.g., colouring, transparency effect, and rendering process) was performed in ZBrush 4R6. When the CT-scan of the Pirro Nord specimen was performed, the distal portion of the premaxillae was taped to the rest of the cranium. Later, the tape and premaxillary fragments were removed for conservation reasons.

Literature data for palaeoneurological analysis were taken from the following Pliocene and Pleistocene taxa of Europe: *Eucladoceros dicranios* [=*Cervus dicranius* in Beccari (1922)] from Castelfiorentino (Italy; Early Pleistocene; Beccari, 1922), *P. nestii* [=*Dama nestii* in Azzaroli and Mazza (1992)] from Olivola (Italy; Early Pleistocene; Azzaroli, 1947), *Cervus warthae* [=*Praeelaphus warthae* in Croitor (2018)] from Węże-1 (Poland; Early Pleistocene; Czyzewska, 1982), *Procapreolus wenzensis* [=*Cervocerus wenzensis* in Czyżewska (1960); =*Procapreolus moldavicus* in Croitor (2018)] from Węże-1 (Poland; Early Pliocene; Czyzewska, 1982), *Megaloceros matritensis* [=*Praedama* in Aguirre and De Andrés (1974)] from Villaverde (Spain; Middle Pleistocene; Aguirre and De Andrés, 1974).

2.5. Statistical analysis

Discriminant analyses were performed to examine the resolution of mesowear and microwear variables. For dental mesowear we used the percentage of high relief, rounded, and blunt cusps as independent variables, and two dietary classifications, "conservative", which includes species with unclear dietary behaviours in the mixed feeder group, and "radical", which pushes them either into the browsers or grazer extremes, as grouping variables (Fortelius and Solounias, 2000). For dental microwear a discriminant analysis was performed using the following independent variables: average number of pits, average number of scratches, percentage of individuals with predominantly fine scratches, percentage of individuals with predominantly coarse scratches, percentage of individuals with a mixture of fine and coarse scratches, percentage of individuals with >4 large pits, percentage of individuals with >4 cross scratches, percentage of individuals displaying gouges. Dietary classification of modern taxa [modified from Solounias and Semprebon (2002)] was used as grouping variables. All analyses were performed using IBM SPSS Statistics 24.

3. Results

3.1. Dental mesowear patterns

The *Dama*-like deer from Pirro Nord displays a mesowear pattern characterised by a marked predominance of high relief (97.4%) and a similar frequency of sharp (51.3%) and round (48.7%) cusps. None of the studied individuals display blunt cusps and only one specimen has a low occlusal relief (SI2), resulting in a low MWS (0.5). These results are consistent with a mixed feeding behaviour leaning towards a higher consumption of soft plant resources. Mesowear discriminant analysis provides a satisfactory dietary discrimination with 74.1% of extant taxa correctly classified according to a conservative (Cons) and radical (Rad) classifications. *Dama*-like deer from Pirro Nord is classified as a mixed feeder in both conservative and radical classifications (Fig. 3; Table 1). These patterns are comparable with those observed in samples of *Dama*-like cervids from the Early Pleistocene localities of Olivola (Villafranchian) and Vallparadís Estació (layer EVT12; Epivillafranchian), respectively (Fig. 3), which are both classified as mixed feeders and display the same MWS values (Table 1).

3.2. Dental microwear patterns

The results of the microwear analysis performed by MicroWeaR are summarized in Table 1. The values refer to the number of pits, scratches, and gouges sampled within the reference area of 0.16 mm^2 of each sample analysed. Observing the average values of the number of pits and scratches, we note a prevalence of the latter compared to pits. Furthermore, coarse scratches are more numerous than fine scratches and large pits are more abundant than small pits. From the comparison with the average number of pits and scratches of the modern ungulate species, it is possible to obtain a first placement of the *Dama*-like deer from Pirro Nord within the trophic categories considered according to the scheme by Solounias and Semprebon (2002).

Dama-like deer from Pirro Nord shows microwear patterns consistent with those of mixed feeders and grazers (Fig. 4). The values of the average number of scratches and pits, in fact, fall close the overlapping area between the seasonal, meal-by-meal mixed, and grazers categories, suggesting a tendency towards a grass-rich diet. These results are consistent with those obtained for Vallparadís Estació layer EVT12. According to microwear results, the *Dama*-like deer from layer EVT7 display instead a less abrasive seasonal mixed diet (Fig. 4; Strani et al., 2019).

Scratch range analysis confirms the result for the *Dama*-like deer from Pirro Nord with a low scratch value of 22.2% falling at the limit between the mixed feeding and grazing range. The most common microwear pattern is comprised of abundant coarse scratches (SWS = 1.6) and large pits (%LP = 100) with gouges being also recorded in some specimens (%G = 27.8) (Table 1). These patterns are observed in most modern grazing ungulates, which exhibit an abundance of coarser features (coarse scratches, large pits, and gouges) compared to leaf browsers and mixed feeders (Solounias and Semprebon, 2002). It also shows a percentage of individuals with a low scratch range equal to 23.80%, falling within the group of mixed feeders (following Solounias and Semprebon, 2002). Finally, only a small number of individuals (4 out of 21) have one or more gouges in the reference area. On the other hand, the number of large pits present in the samples is quite high in almost all individuals, compared to the small pits which are in much smaller numbers (Table 1).

Discriminant analysis performed using all microwear variables classify the *Dama*-like deer from Pirro Nord as a fruit browser (72.2% correctly classified modern taxa, 47.7% in cross-validation) even when

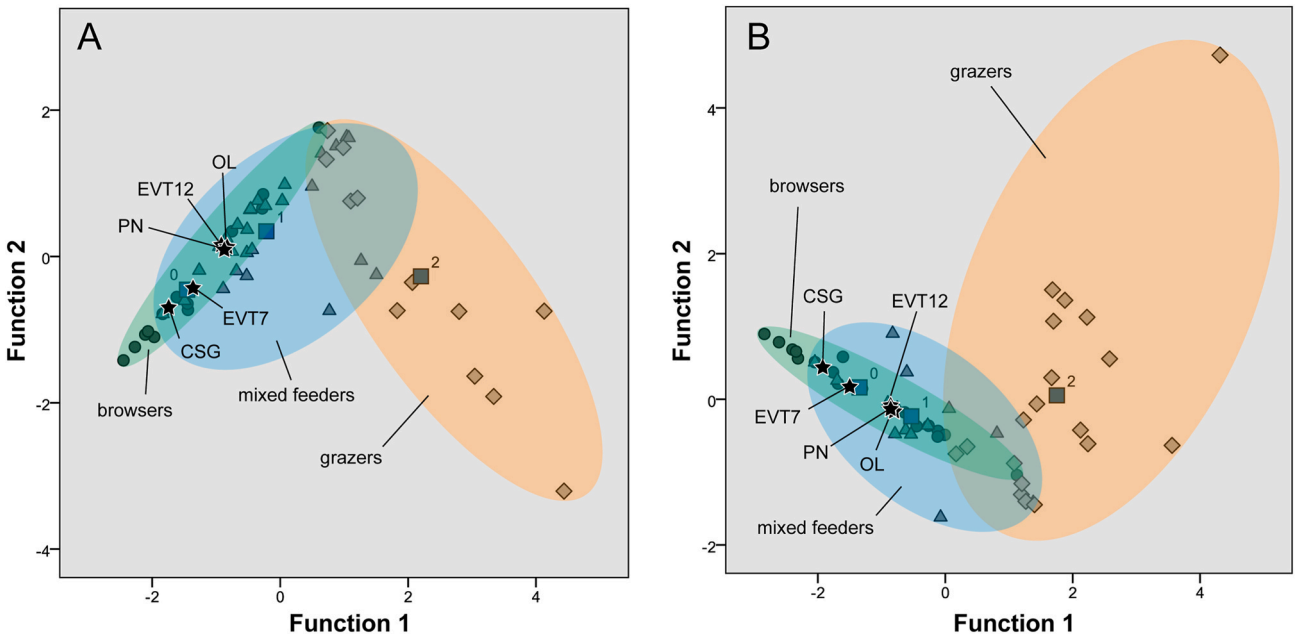

Fig. 3. Results of the CVA based on three extant dietary categories and mesowear variables. Results based on dietary conservative (A) and radical (B) classifications. The radical assignment of the species informs about a possible foraging specialisation (i.e., dietary tendency) of the mixed feeder species. Data on extant species are from Fortelius and Solounias (2000). Abbreviations: Olivola (OL); Coste San Giacomo (CSG); EVT7 (EVT7) and EVT12 (EVT12) layers of Vallparadís Estació; Pirro Nord (PN). Large square symbols denote group centroids.

Table 1
Summary of dental mesowear and microwear analysis. Abbreviations (mesowear): number of specimens measured (N); percentage of specimens with high (%High) and low (%Low) occlusal relief; percentage of specimens with sharp (%Sharp), rounded (%Round), and blunt (%Blunt) cusps; mesowear score (MWS). Predicted diets according to a conservative (CONS) and radical (RAD) mesowear classification. Abbreviations (microwear): average number of pits (AP); average number of scratches (AS); percentage of individuals with >4 large pits (%Lp); percentage of individuals with gouges (%G); percentage of individuals with >4 cross scratches (%XS); scratches width score (SWS); percentage of specimens with between 0 and 17 scratches (%0–17); percentage of individuals with predominantly fine scratches (%FS); percentage of individuals with a mix of fine and coarse scratches (%MS); percentage of individuals with predominantly coarse scratches (%CS). *Extant seasonal and non-seasonal mixed feeders are grouped together into a single dietary category referred to as "mixed feeders".

	Mesowear							Predicted Diet					
Locality	**N**	**% High**	**% Low**	**% Sharp**	**% Round**	**% Blunt**	**MWS**	**CONS**	**RAD**				
Pirro Nord	39	97.4	2.6	51.3	48.7	0.0	0.5	Mixed Feeder	Mixed Feeder				
Vallparadís Estació (EVT7)	34	97.1	2.9	67.6	32.4	0.0	0.4	Browser	Browser				
Vallparadís Estació (EVT12)	10	100.0	0.0	50.0	50.0	0.0	0.5	Mixed Feeder	Mixed Feeder				
Olivola	36	97.2	2.8	50.0	50.0	0.0	0.5	Mixed Feeder	Mixed Feeder				
Coste San Giacomo	26	100.0	0.0	76.9	23.1	0.0	0.2	Browser	Browser				
	Microwear											**Predicted Diet**	
Locality	**N**	**AP**	**AS**	**%LP**	**%G**	**%XS**	**% 0–17**	**SWS**	**%FS (0 SWS)**	**%MS (1 SWS)**	**%CS (2 SWS)**	**Type**	**Type***
Pirro Nord	18	18.9	25.8	100	27.8	11.1	16.7	1.6	0.0	44.4	55.6	Fruit Browser	Fruit Browser
Vallparadís Estació (EVT7)	14	14.5	17.8	50.0	21.4	14.3	57.1	0.1	85.7	14.3	0.0	Seasonal Mixed Feeder	Seasonal Mixed Feeder
Vallparadís Estació (EVT12)	3	20.0	26.5	33.3	66.7	0.0	0.0	0.0	100.0	0.0	0.0	Seasonal Mixed Feeder	Seasonal Mixed Feeder

extant seasonal and non-seasonal mixed feeders are grouped together in a single dietary classification (mixed feeder) 77.3% correctly classified modern taxa, 61.4% in cross-validation) (Table 1; Fig. 5). This discrepancy between the mesowear results and information from single microwear variables (such as average number of scratches) may be explained by the relatively abundance of coarse features (%LP = 100; SWS: 1.6) which is also commonly recorded in bark eaters and browsing animals that feed mostly on fruits (Solounias and Semprebon, 2002).

3.3. Stable isotopes

The enamel bioapatite $\delta^{13}C$ values of material from Pirro Nord range between −11.49 ‰ and −13.10 ‰, which is equivalent to the ranges between 25.49 ‰ and 27.10 ‰ in plant diet or ecosystem values, whereas the $\delta^{18}O$ values vary from −2.05 ‰ to −6.80 ‰ (VPDB) and from 28.74 ‰ to 23.85 ‰ (SMOW) (Table 2). The percentage of C4 plants in the diet of this deer was very low, with only one specimen showed about 8% of C4 consumption. The other two were consuming C3

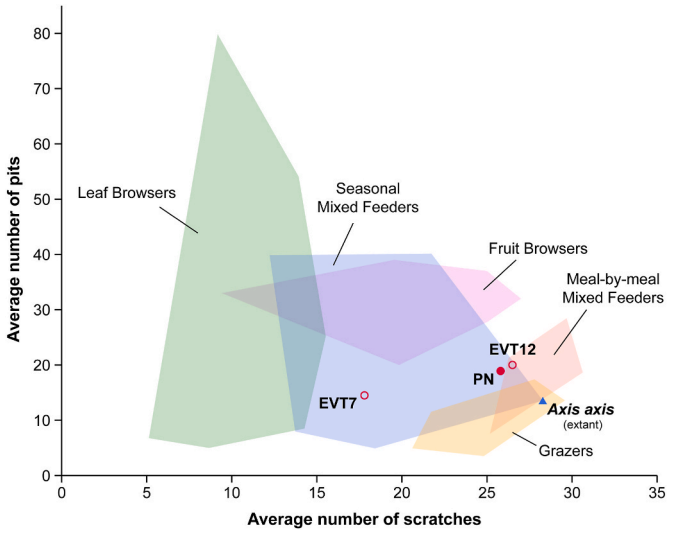

Fig. 4. Scatter plot of the average number of pits and scratches for modern ungulate species, *Dama*-like cervids from Pirro Nord (PN) and layers EVT7 and EVT12 of Vallparadís Estació. Modern species are divided into the categories of fruit browsers, leaf browsers, mixed feeders who vary the diet from meal to meal, mixed feeders who vary the diet on a seasonal-regional basis, and grazers, according to the scheme of Solounias and Semprebon (2002).

plants. The studied specimens demonstrated temperature variations between 9.2 °C and 16.7 °C. (Table 2).

3.4. Description of external morphology

3.4.1. Cranium

The male cranium DE 11-1/ind.A (Fig. 6) is in very good state of preservation, missing only the right zygomatic arch and a small rostral portion of the splanchnocranium on the right side. The right orbit is slightly compressed dorsoventrally. Cranial sutures are all well visible, especially the interfrontal and frontoparietal ones, which are deeply invaginated. The base of the right antler including the basal tine, is still attached to the cranium, whereas the remaining part of the antler is preserved separately. The left antler is also nearly complete but separated from the cranium due to a fracture at about mid height of the pedicle.

In lateral view, the braincase is relatively short and rounded, with bulging parietal and frontal dorsal outlines forming an obtuse angle. The temporal fossa is wide, anteroposteriorly elongated, and with convex surface. Posteriorly, the Akrokranion extends more backwards than the posterior margin of the occipital condyles. The external auditory meatus is directed posterodorsally. The paraoccipital process extends more ventrally than the ventral margin of the tympanic bulla.

Anteriorly to the pedicle, the frontal slopes steeply forming a sharp forehead, which rises obliquely above the orbit. The pedicle is slightly inclined posteriorly. The left zygomatic arch is thin and slightly inclined towards the toothrow. Posteriorly to the zygomatic arch and in continuity with it, a strong sub-horizontal crest develops reaching posteriorly the occipital squama. The pterygoid is inclined in anteroventral direction. The postorbital bar is inclined by about 45° compared to the sagittal axis, it constitutes a strong posterior orbital margin, and its posterior face is deeply excavated by the parietal. The orbit is very wide

Table 2
Isotopic results for the *Dama*-like deer from Pirro Nord. Abbreviations: "Vienna PeeDee Belemnite" (VPDB) and "Vienna Standard Mean Ocean Water" (VSMOW) international reference standard for the carbon and oxygen.

ID	Tooth	$\delta^{13}C$(VPDB)	$\delta^{18}O$ (VPDB)	$\delta^{18}O$ (SMOW)
GP 23	M2 dx	−13.1	−2,05	28.74
GP 28	M2 dx	−12.41	−6.8	23.85
GP 32	M2 dx	−11.49	−6	24.67
ID	**Tooth**	**$\delta^{18}OPh$**	**$\delta^{18}OW$**	**Temperature, °C**
GP 23	M2 dx	19.72	−5.16	16.7
GP 28	M2 dx	15	−9.34	9.2
GP 32	M2 dx	15.79	−8.64	10.5

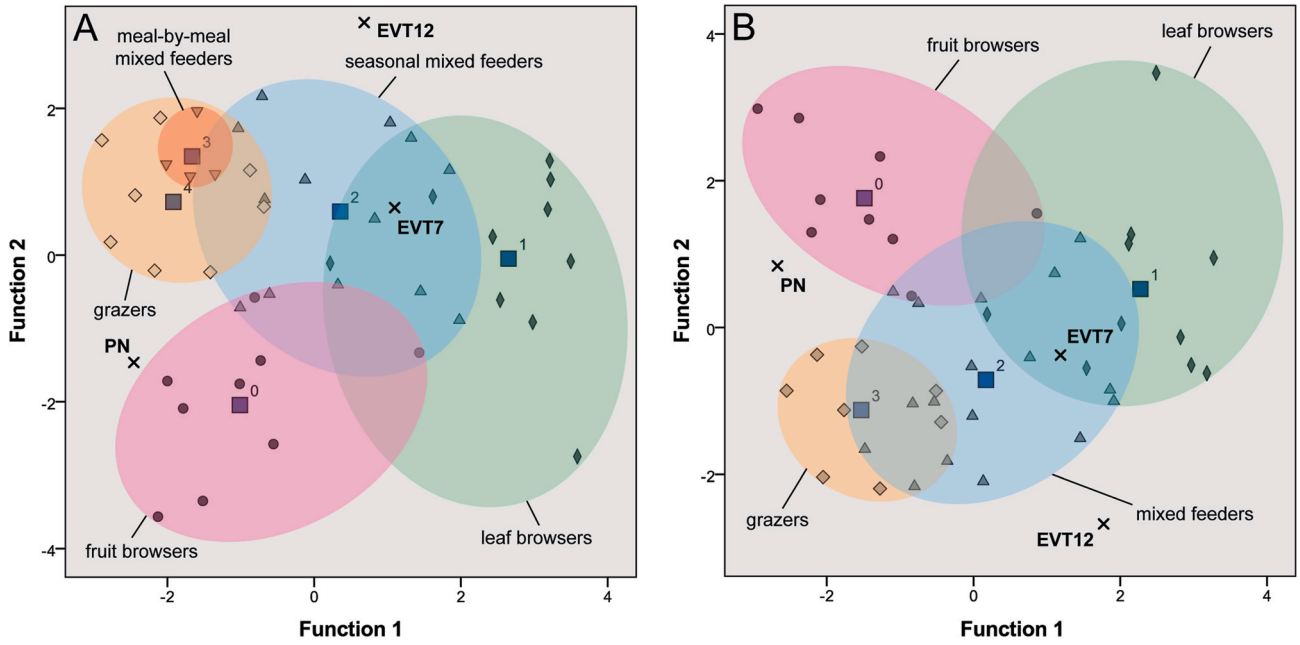

Fig. 5. Bivariate diagrams based on discriminant analysis performed with microwear data. A, Classification using extant ungulate dietary types as grouping variables: fruit browsers (0); leaf browsers (1); seasonal mixed feeders (2); meal-by-meal mixed feeders (3); and grazers (4). B, Classification grouping extant seasonal and non-seasonal mixed feeders in a single dietary category (mixed feeders): fruit browsers (0); leaf browsers (1); mixed feeders (2); and grazers (3). Square symbol indicates group centroids. Extant ungulates data are from Solounias and Semprebon (2002). Abbreviations: *Dama*-like cervids from Pirro Nord (PN) and Vallparadís Estació layers EVT7 (EVT7) and EVT12 (EVT12).

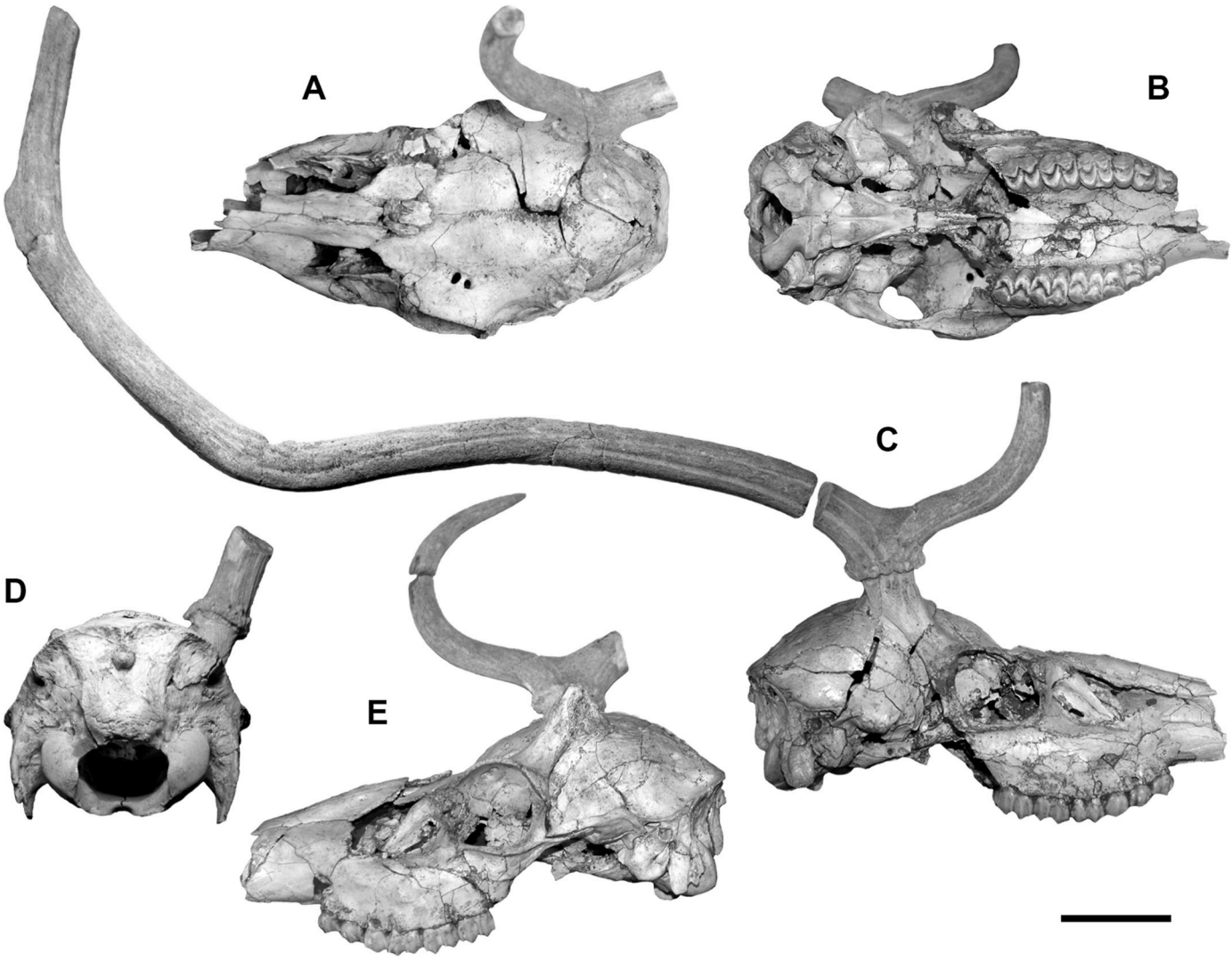

Fig. 6. *Dama*-like deer from Pirro Nord, cranium DE 11-1/ind.A in dorsal (A), ventral (B), right lateral (C), posterior (D), and left lateral (E) views. In C, the right antler is shown in its anatomical position according to the reconstruction of the antlered cranium of Croitor (2014). Scale bar: 5 cm.

and rounded, and two lacrimal foramina are clearly visible on its anterior margin. Anteriorly to the orbit, a deep and triangular preorbital fossa is present. The ethmoidal vacuity (incomplete on the right side and with fragmented anterior margin on the left) is separated from the preorbital fossa by a sharp oblique crest. The ethmoidal vacuity is slightly wider than the preorbital fossa. The maxilla is stout and with an overall convex lateral surface. A distinct facial tuber develops above the M1 at about mid height on the maxilla. The infraorbital foramen is wide and opens above the mesial margin of the P2. The muzzle is slender and elongated, exceeding the length of the neurocranium. The dorsal margin of the nasal is slightly convex. The incisive bone is elongated and pointed, with relatively wide nasal process inclined by about 45° compared to the sagittal axis.

In dorsal view, the neurocranium shows a trapezoidal posterior outline, whereas the splanchnocranium appears elongated and tapered. The pedicles are divergent each other (i.e., directed outwards). The pedicle section is roughly circular. The orbits are oriented anterolaterally, forming an angle of about 30° with the sagittal axis. Two large supraorbital foramina are located at about mid length of the orbit, opening within a shallow furrow parallel to the lateral orbital border. The frontals are slightly concave in the area between the supraorbital foramina and the base of the pedicles; conversely, they appear convex between the orbits and especially between the pedicles, where they form a shallow interfrontal crest. Although the posterior portion of the nasals is broken, they seem to end approximately at mid length of the ethmoidal vacuity. The (left) incisive bone shows a lateral enlargement at the level of the posterior end of the palatine fissure.

In posterior view, the foramen magnum is elliptical (i.e., wider than high). The occipital squama is shaped as an almost perfect semicircle. It is divided medially by a strong vertical bulge approximately as wide as the foramen magnum, running ventrally from the latter up to the external occipital protuberance. The latter is represented by a distinct circular button-like bulge. Two smaller crest-like bulges develop at the dorsolateral corners of the occipital squama, about at the same height of the external occipital protuberance. The mastoid processes are quite weak, whereas the paraoccipital processes are strong, ventrally pointed, and higher than the ventral margin of the basioccipital.

In ventral view, the cranium appears overall elongated and slender. The basioccipital is wide posteriorly, pointed anteriorly, and with convex surface. Posteriorly, the basilar part of the occipital condyles is massive. Anteriorly, the bone is crossed by a deep sagittal furrow, which separates the two bulging and elongated occipital tubercles. The basisphenoid is pointed anteriorly and delimited laterally by high and sharp pterygopalatine crests. The suture between the basioccipital and basisphenoid is straight. Lateral to the suture, prominent pterygoid crests develop. The tympanic bullae are swollen and elongated in

anteromedial to posterolateral direction. Posterior to the bullae, the paraoccipital processes are elongated and slightly converging each other. The glenoid cavities are wide and convex and are delimited posteriorly by strong retroarticular processes. The palatine laminae are poorly preserved and delimit laterally narrow choanae. The palate is long and narrow, having a length approximately the same as that of the neurocranium and a width that is less than half the bizygomatic width. No palatine foramina are visible.

3.4.2. Antlers

The antlers of DE 11-1/ind.A are almost entirely preserved and morphologically correspond to a young adult ontogenetical state. They have only two tines: a basal tine and a terminal one. The latter represents the anterior tine of a terminal fork, which is poorly developed as its posterior tine is reduced to a small bump on each side. A middle (trez) tine lacks. The basal tine is positioned right above the burr and forms an obtuse angle with the beam. The tine branches towards the anterolateral direction forming a narrow angle with the sagittal axis of the cranium. It is directed slightly anterodorsally in its lower part and then it steeply curves more upwards becoming almost vertical. The terminal fork opens about two thirds of the length of the beam. Although the posterior tine is weakly developed, the fork is almost parallel to the sagittal axis of the cranium. The anterior tine is moderately long and directed anterodorsally. In lateral view, from bottom to top, the beam is directed posterodorsally, then it bends slightly downwards to sharply turns upwards at about mid length, and finally forwards in its upper part. In anterior view, the beam starts right but early bends laterally for the first third of its length, it turns upwards at about mid length to be directed medially in correspondence to the terminal fork. The sections of the beam and tines are sub-circular in almost all of their development, except near the bifurcations where they flatten slightly. Shallow longitudinal grooves run along the entire antler but are particularly visible in the intermediate part of the beam, right below the terminal fork. Comparison of antler measurements with those of other Villafranchian and Epivillafranchian *Dama*-like cervids are provided in SI3, where a greater similarity can be observed with material from Le Vallonnet, although with some differences in size and proportions (i.e, shorter and slenderer pedicles in the Pirro Nord sample; SI3a-b).

3.4.3. Teeth

The upper cheek teeth are all preserved and in moderate stage of wear. The lingual walls of the M2 and M3 are rough, while those of all other teeth are smooth. In occlusal view, the P2 is smaller than the P3, but they have similar general morphology. The mesial margin of the P2 is very swollen. Both the P2 and P3 exhibit an incipient molarization, that is, a lingual notch (deeper in the P2) separating the tooth into a mesial and a distal lobe (protocone and hypocone, respectively). The parastyle, mesostyle, and especially metastyle have pointed margins. The P4 is mesiodistally compressed, and with less pointed labial styles. It possesses a distolingual cingulum. In all premolars, the central cavities are well developed and shows enamel folds especially along the lingual outline. In all premolars, a small transversal enamel islet develops very close to the distal margin of the teeth (in fact, in some of them, this islet opens towards the distal wall of the tooth.

The upper molars show an overall squared occlusal outline. The mesiolingual and lingual cingula are present but weak in all molars. The lingual cingulum culminates in the middle with a well-developed entostyle. The lingual lobes are rounded in the M1 due to the more advanced wear, whereas they are more triangular in the M2 and M3. The central cavities of the molars are V shaped and have enamel folds on their distolingual edges. Labially, the cusps and styles are very projecting, with the parastyle showing a characteristic bending towards the distal direction (i.e., comma shaped). Comparison of tooth measurements with those of other Villafranchian and Epivillafranchian *Dama*-like deer samples are provided in SI4. Pirro Nord teeth display somewhat different size and proportions compared to Le Vallonnet and Olivola samples, particularly in lower fourth premolars (SI4a), lower first molars (SI4b), and lower third molars (SI4c).

3.5. Brain description

The virtual endocast obtained from DE 11-1/ind.A cranium consists of a complete brain with both olfactory bulbs, a globose and dorsally curved cerebrum, the cerebellum and a portion of the brain stem (Figs. 7 and 8). The overall morphology of the olfactory bulbs is well-preserved despite their rostral portion, corresponding to the anterior ramifications, are missing. In dorsal view, the peduncles of the olfactory bulbs diverge with a V-shaped angle. The cerebrum is large (see Table 3 for the complete list of measurements) and in lateral view shows a dome-shaped outline. In dorsal view, the frontal lobes are narrower compared to the temporal ones forming a constriction at the level of the sylvian fissure (lateral sulcus). From front to back, a marked longitudinal fissure divides the cerebrum in two roughly symmetrical hemispheres. The convolutions are barely pronounced on the parietal and occipital lobes where some reduced portions of the lateral, ectolateral, and suprasylvian sulci are recognizable (Figs. 7 and 8). The cerebellum is compact with a poorly marked vermis which appears mostly covered by the occipital lobe of the brain, especially in dorsal view. The brain stem and the main cranial nerves are well preserved (see Fig. 8 for the complete list).

4. Discussion

4.1. Palaeoecology

Mesowear analysis points to a long-term mixed diet for the *Dama*-like deer of Pirro Nord with the lack of blunt cusps and low occlusal relief, suggesting a low consumption of abrasive food (Table 1). The range of the stable isotope $\delta^{13}C$ ratios suggest that it was a mixed feeder foraging almost exclusively on abrasive water stressed C3 vegetation in warm woodland and semi-open habitats although the observed range of $\delta^{13}C$ values does not necessary imply the absence of C4 vegetation, but simply reflect a dietary preference of the sampled individuals. High $\delta^{18}O$ values indicate the ingestion of water from vegetation also pointing to adaptations to arid environments.

Microwear analysis, which records the short-term diet, suggests a mixed diet with a strong tendency towards a grazing behaviour, as indicated by the relative abundance of scratches observed on the analysed teeth (Table 1), which in modern taxa are usually associated with consumption of abrasive items, such as grasses (Solounias and Semprebon, 2002). The simultaneous presence of a high number of pits (Table 1), which in modern ungulates is typically linked to a more selective diet (Solounias and Semprebon, 2002), indicates that the *Dama*-like deer from Pirro Nord also integrated other food types in its diet. By plotting average number of pits and scratches, the Pirro Nord sample falls within the range of variability of mixed feeders overlapping with grazers, close to the data of the modern chital *A. axis* (Fig. 4). *Axis* is widespread in India, Nepal, and Sri Lanka and lives in transitional habitats between the forest and the prairie areas displaying eating habits which tend towards grazing, although it can also integrate fruits, leaves, and shoots in its diet based on seasonal or regional availability (Moe and Wegge, 1994; Grubb, 2005).

Interestingly, a high percentage of individuals displaying an abundance of coarse features (coarse scratches and large pits, in particular) is also recorded, a condition which is usually observed in modern fruit browsers (Solounias and Semprebon, 2002). Large pits, especially if associated with a high number of coarse scratches, can be however also attributed to the chewing of grit-infested food a condition commonly observed in ungulates that feed in arid environments, where both foliage and herbaceous plants are often covered with sand, dust, and debris (Williams and Kay, 2001; Solounias and Semprebon, 2002; Kaiser, 2009). For instance, browsing animals that feed on grit-infested plant

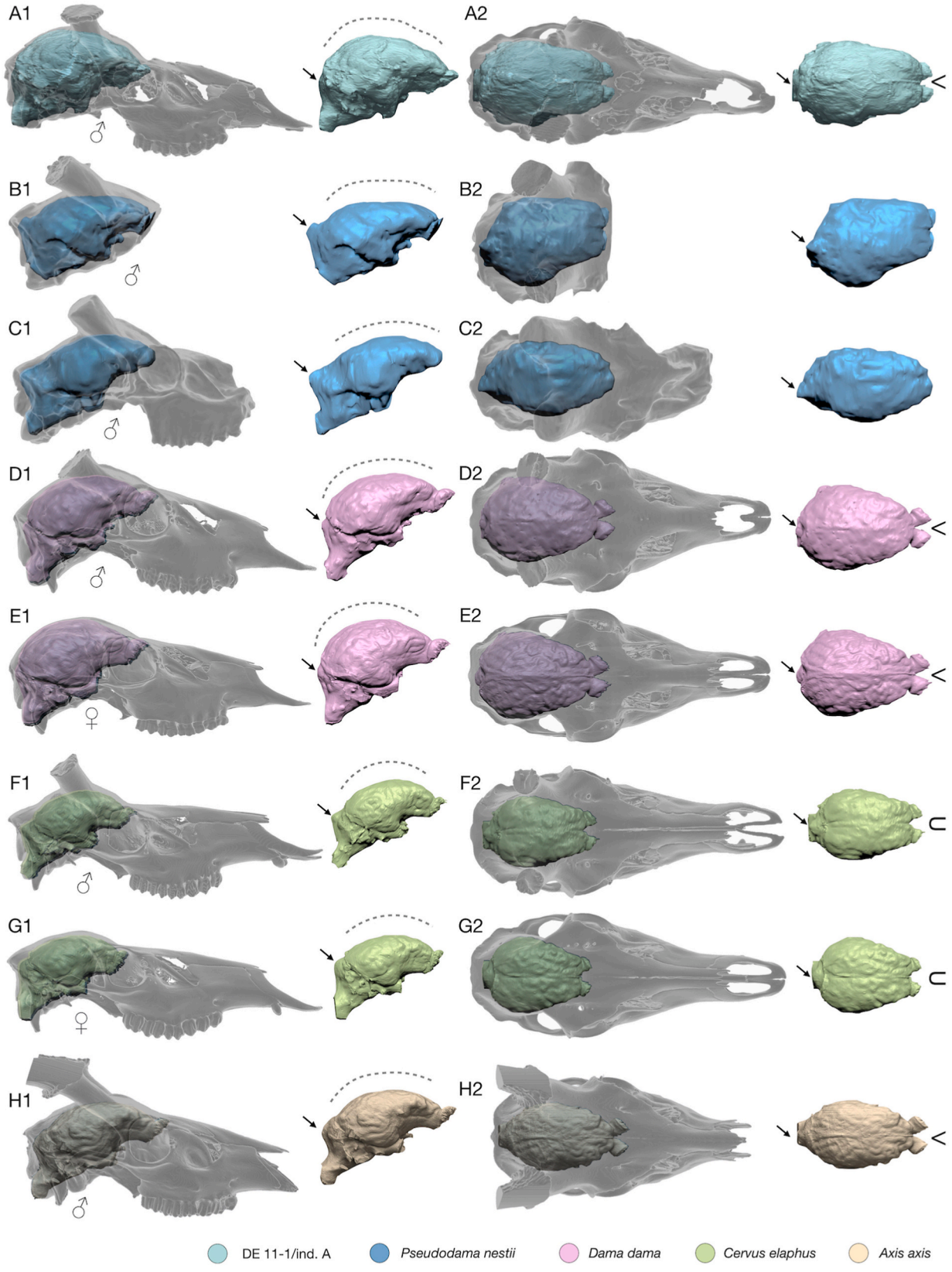

Fig. 7. CT-based comparison of crania and brain endocasts. (**A**) male DE 11-1/ind.A *Dama*-like deer from Pirro Nord; (**B**) *P. nestii*, male SABAP_UMB 337643 from Pantalla; (**C**) *P. nestii*, male SABAP_UMB 337655 from Pantalla; (**D-E**) extant *Dama*, male CZUFLD FaD002 (**D**) and female CZUFLD FaD003 (**E**); (**F-G**) extant *Cervus elaphus*, male CZUFLD ReD002 (**F**) and female CZUFLD ReD003 (**G**); (**H**) extant *Axis*, male MCN 3310. Crania and brains in right lateral (**A1–H1**) and dorsal (**A2–H2**) views. The black arrows indicate the prominence of the cerebellum, the dotted lines indicate the dorsal curvature of the cerebrum, while symbols on the right indicate the V or U shape of the olfactory bulbs. All the images are normalized.

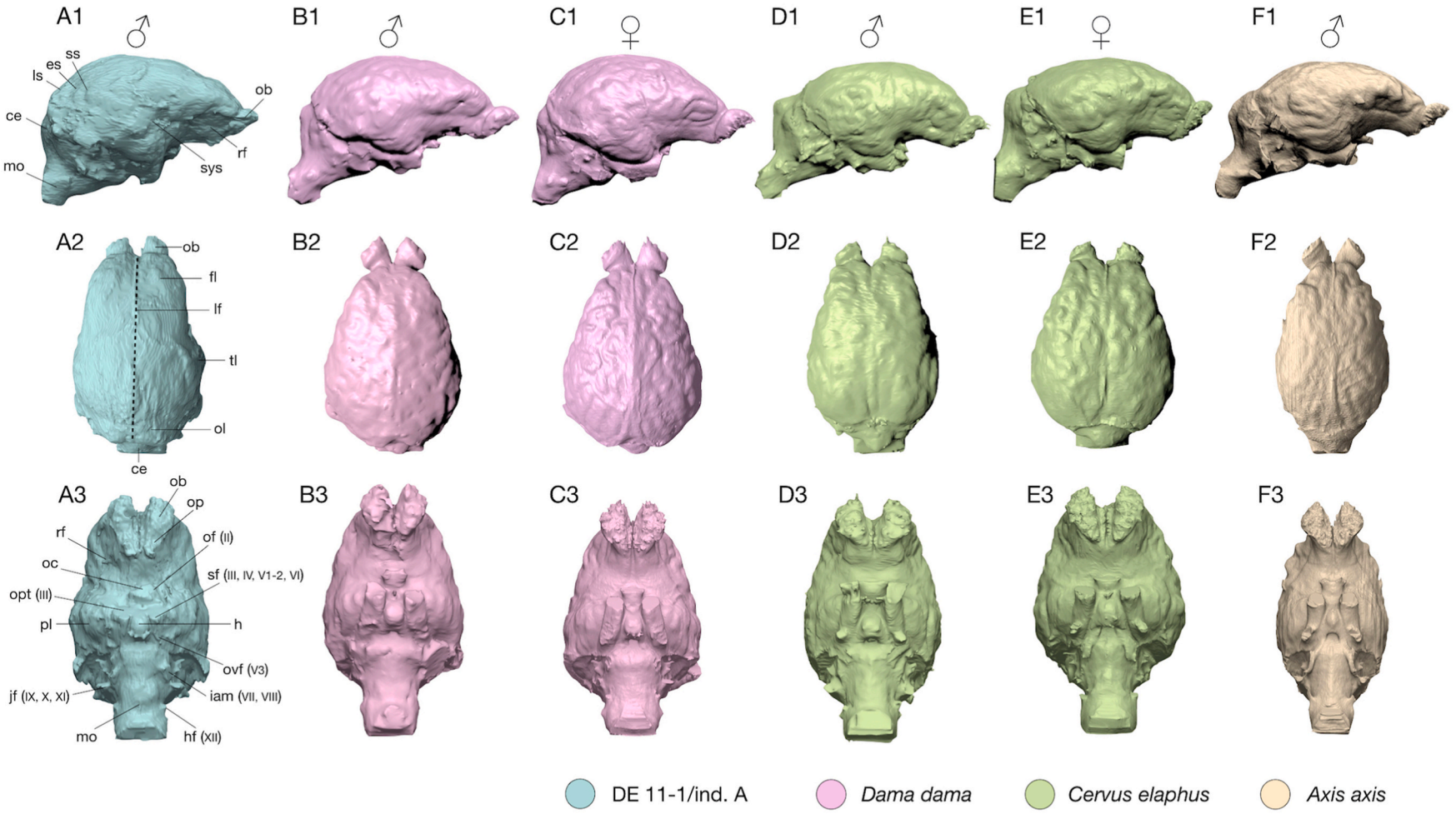

Fig. 8. Comparison of brain endocasts. (**A**) male DE 11-1/ind.A *Dama*-like deer from Pirro Nord; (**B-C**) extant *Dama*, male CZUFLD FaD002 (**B**) and female CZUFLD FaD003 (**C**); (**D-E**) extant *Cervus elaphus*, male CZUFLD ReD002 (**D**) and female CZUFLD ReD003 (**E**); (**F**) extant *Axis*, male MCN 3310. Brains in right lateral (**1**), dorsal (**2**), and ventral (**3**) views. Abbreviations: **ce**, cerebellum; **es**, ectolateral sulcus; **fl**, frontal lobe; **h**, hypophysis; **hf**, hypoglossal foramen; **iam**, internal acoustic meatus; **jf**, jugular foramen; **lf**, longitudinal fissure; **ls**, lateral sulcus; **mo**, medulla oblongata; **ob**, olfactory bulb; **oc**, optic chiasm; **of**, optic foramen; **ol**, occipital lobe; **op**, olfactory peduncle; **opt**, optic foramen; **ovf**, oval foramen; **pl**, pyriform lobe; **rf**, rhinal fissure; **sf**, sphenorbital fissure; **ss**, suprasylvian sulcus; **sys**, sylvian sulcus; **tl**, temporal lobe. All the images are normalized.

Table 3
Selected measurements of the brain of DE 11-1/ind.A compared with extinct (*Pseudodama nestii*, *Eucladoceros dicranios, Cervus warthae, Procapreolus wenzensis*, and *Megaloceros matritensis*) and extant (*Dama*, *Cervus elaphus*, and *Axis*) deer. Total brain volume (**BV**) as represented in Fig. 8, length of the telencephalon (**TeL**), breadth of the telencephalon (**TeB**).

Species	Catalgue number	Age	Locality	Gender	BV (mm)3	TeL (mm)	TeB (mm)	TeB/L	References
"Dama-like" deer	DE 11-1/ind. A	Early Pleistocene	Pirro Nord (Italy)	Male	289,732.67	108.08	76.26	0.7	This work
Pseudodama nestii	SABAP_UMB 337643	Early Pleistocene	Pantalla (Italy)	Male	197,408.86	94.42	66.24	0.70	Cherin et al. (2022)
Pseudodama nestii	SABAP_UMB 337655	Early Pleistocene	Pantalla (Italy)	Male	200,667.41	94.17	74.72	0.79	Cherin et al. (2022)
Pseudodama nestii		Early Pleistocene	Olivola (Italy)	/	/	~ 100-110	~ 80	0.80-0.72	Azzaroli, 1947
Eucladoceros dicranios		Early Pleistocene	Castelfiorentino (Italy)	/	/	119	98	0.82	Beccari (1922)
Cervus warthae	MZVIII-Vn-362/1	Early Pliocene	Węże-1 (Poland)	/	/	/	67.7	/	Czyzewska, 1982
Cervus warthae	MZVIII-Vn-362/4	Early Pliocene	Węże-1 (Poland)	/	/	104	/	/	Czyzewska, 1982
Cervus warthae	MZVIII-Vn-362/370	Early Pliocene	Węże-1 (Poland)	/	/	~75	74	0.98	Czyzewska, 1982
Procapreolus wenzensis	MZVIII-Vn-361/3	Early Pliocene	Węże-1 (Poland)	/	/	~78	54	0.69	Czyzewska, 1982
Megaloceros matritense		Middle Pleistocene	Villaverde (Spain)	Male	/	108	92.5	0.85	De Andres and Aguirre, 1974
Dama	CZUFLD FaD001	Extant		Male	258,964.94	97.93	74.73	0.76	Cherin et al. (2022)
Dama	CZUFLD FaD002	Extant		Male	226,033.66	96.13	72.26	0.75	Cherin et al. (2022)
Dama	CZUFLD FaD003	Extant		Female	228,506.55	92.55	71.42	0.77	Cherin et al. (2022)
Cervus elaphus	CZUFLD ReD001	Extant		Male	343,561.22	102.65	84.23	0.82	Cherin et al. (2022)
Cervus elaphus	CZUFLD ReD002	Extant		Male	353,098.89	104.27	83.37	0.80	Cherin et al. (2022)
Cervus elaphus	CZUFLD ReD003	Extant		Female	307,260.02	98.91	83.21	0.84	Cherin et al. (2022)
Axis	MCN 3310	Extant		Male	197,285.74	93.53	64.55	0.69	Fontoura et al. (2020)

resources may display a microwear pattern comprised of coarser scratches, heavy pitting and gouges (Solounias and Semprebon, 2002). The dietary abrasiveness in the sample of Pirro Nord may thus be a result of a "dirty" feeding behaviour which can explain why this deer is classified as a fruit browser when the discriminant analysis is performed with microwear variables (Fig. 5). A grit-infested grass-rich mixed diet better explain the obtained results, a hypothesis which is consistent with the palaeoenvironmental and palaeoclimatic reconstructions of Pirro Nord based on the study of other vertebrate groups such as reptiles and amphibians (Blain et al., 2019) and birds (Bedetti and Pavia, 2013), which indicate that the site was dominated by wide open grasslands interspersed with wetter areas with higher vegetation and greater water availability.

Considering the available data on the ecology of other Early Pleistocene cervids, it is possible to observe a trend in their feeding behaviours towards increasingly more abrasive diets (Strani, 2021). Early Villafranchian *Dama*-like deer display dental wear patterns compatible with a browsing diet [e.g., at Coste San Giacomo; Strani et al. (2015)], whereas those from the early late Villafranchian show dental wear pattern consistent with a diet richer in herbaceous resources [e.g., *P. nestii* at Olivola; Strani et al. (2018a)]. In this context, the *Dama*-like deer from Pirro Nord may represent a further step towards an even pronounced adaptation of this group on consumption of abrasive plants in more arid habitats. This scenario is also consistent with the gradual process of aridification of the environmental conditions that occurred in the Early Pleistocene following the onset of the Quaternary glaciations at the Plio-Pleistocene transition which in the European continent led to the extirpation of sub-tropical biomes and to the expansion of prairies (Fortelius et al., 2006; Combourieu-Nebout et al., 2015; Head and Gibbard, 2015). Duval et al. (2024) have recently suggested a possible younger age (~0.8 Ma) for Pirro Nord, that is, within the Epivillafranchian and closer to Vallparadís Estació layer EVT7 (0.858 ± 0.087 Ma). If this new age is accepted, it cannot be excluded that the *Dama*-like deer from Pirro Nord, Vallparadís Estació, and other Epivillafranchian localities (e.g., Le Vallonnet) may belong to the same species. In this scenario the differences observed between the Italian and Iberian deer around 0.8 Ma in terms of dietary behaviours (grass-rich "dirty" mixed diet at Pirro versus browse-rich seasonal mixed diet at EVT7) and environmental context (generally arid with sparse vegetation at Pirro versus less arid conditions with a seasonal high availability of heterogeneous plant resources at EVT7; Strani et al., 2019) may thus indicate a high degree of plasticity that allowed this deer to successfully occupy diverse habitats.

4.2. Palaeoneurology

Neuroanatomy of fossil Cervidae is still largely unexplored and based on a limited number of studies some from the first half of the last century (e.g., Beccari, 1922; Azzaroli, 1947; Aguirre and De Andrés, 1974 and the literature therein; Czyzewska, 1982; Fontoura et al., 2020). Only recently, Cherin et al. (2022) provided a CT-based description of two virtual endocasts of *P. nestii* from the Early Pleistocene site of Pantalla.

Compared to the previously published endocasts, the sample from Pirro Nord stands out for its completeness and good state of preservation, despite the convolutions are only partially detectable. The cerebrum is anteroposteriorly elongated and exceeds in length those of other fossil and extant specimens considered in this work, except for *E. dicranios* from the Early Pleistocene of Castelfiorentino (Italy; Beccari, 1922) and *M. matritensis* (Van der Made, 2019) from the Middle Pleistocene of Villaverde (Spain; Aguirre and De Andrés, 1974) (Table 3). The cerebrum width is narrower than those reported for *E. dicranios*, *M. matritensis*, and *C. elaphus*, with values similar to those of *D. dama* and those of the analysed *P. nestii* and *C. warthae* specimens. Considering the proportions (i.e., ratio between the breadth and length of the cerebrum), the specimen DE 11-1/ind.A matches the values of *P. nestii*, *Pr. wenzensis*, *D. dama*, and *A. axis*. In the *Dama*-like cervid from Pirro Nord the brain volume is larger compared to extant *D. dama* and *P. nestii* from Pantalla, but the two specimens from Pantalla are poorly preserved and both lack the olfactory bulbs. The brain volumes of *C. elaphus* exceed those of the whole sample, although this could be due to the overall larger body size of this species compared to the other taxa.

In terms of general morphology, the specimen from Pirro Nord shares with the extant *Dama* a dorsally curved cerebrum and a compact cerebellum with a poorly marked vermis. In contrast, the fossil samples from

Pantalla, Olivola, Węże-1, and Castelfiorentino, as well as the extant *C. elaphus* and *A. axis*, show a more dorsoventrally flattened cerebrum and a prominent cerebellum with a marked vermis (Figs. 7 and 8). Moreover, the specimen DE 11-1/ind.A shares with the extant *Dama* and *Axis* a V-shaped margin between the olfactory bulbs, whereas in present-day *Cervus* it appears U-shaped.

These features make the Pirro Nord material morphologically very close to the present-day *Dama*. The hypothesis that dorsoventrally compressed cerebra represent a primitive character in Cervini (at least in Pleistocene European forms) was suggested by Azzaroli and Mazza (1992) and supported by Cherin et al. (2022). The latter authors have pointed out that the early Pleistocene *P. nestii* displays a mosaic of intermediate characters between extant *Dama* and *Cervus*, but with a prevailing resemblance to *Dama*. This condition would appear to be even more pronounced in the late Early Pleistocene *Dama*-like deer from Pirro Nord, suggesting that "*Dama*-like features" were developed in brain morphology during the Early Pleistocene. Considering these neuroanatomical similarities, it would be reasonable to assume that the cognitive abilities of the Pirro Nord deer were probably similar to those of the extant *Dama*. But to evaluate this hypothesis and to understand whether these brain features were driven by phylogenetic factors or may reflect a response to the gradual environmental and ecological changes that occurred in the Early Pleistocene, further analyses on a larger fossil sample are needed.

5. Conclusions

The palaeoecological and palaeoneurological analysis of the late Early Pleistocene *Dama*-like deer from Pirro Nord provides clues on the evolutionary trends of this group. The Pirro Nord specimens display the most evident adaptations for grass-rich diet in open habitats compared to other *Dama*-like cervids from Iberian and Italian localities, suggesting that the high dietary versatility of this group was the key factor that allowed it to survive the drastic reduction and subsequent disappearance of subtropical habitats in Europe following the onset of the Quaternary glacial cycles. The neuroanatomy of the Pirro Nord cranium compared with that of other extinct and extant cervids suggests that this group gradually developed "*Dama*-like" features at least in terms of brain morphology, with specimen from Pirro Nord displaying the closest affinity to modern fallow deer. If this is evidence that Late Villafranchian and Epivillafranchian forms may belong to the fallow deer evolutionary lineage as proposed by Croitor (2018), or if instead it is evidence of evolutionary convergence between *Dama* and an extinct genus (e.g., *Pseudodama*), needs to be tested with a larger set of both Early Pleistocene fossils with well-defined craniodental features, and modern and fossil specimens of *Dama*.

CRediT authorship contribution statement

Flavia Strani: Conceptualization, Methodology, Validation, Formal analysis, Investigation, Resources, Data curation, Writing – original draft, Writing – review & editing, Visualization, Funding acquisition. **Francesca Di Folco:** Formal analysis, Data curation, Writing – original draft. **Dawid Adam Iurino:** Formal analysis, Investigation, Resources, Data curation, Writing – original draft, Writing – review & editing, Visualization. **Marco Cherin:** Formal analysis, Resources, Writing – original draft, Writing – review & editing, Visualization. **Diana Pushkina:** Formal analysis, Investigation, Data curation, Writing – review & editing. **Lorenzo Rook:** Resources, Writing – review & editing. **Raffaele Sardella:** Resources, Writing – review & editing. **Beatriz Azanza:** Formal analysis, Investigation, Resources, Writing – review & editing, Supervision. **Daniel DeMiguel:** Methodology, Writing – review & editing, Supervision.

Declaration of competing interest

The authors declare that they have no known competing financial interests or personal relationships that could have appeared to influence the work reported in this paper.

Data availability

Dental meso- and microwear data are available as Supplementary Information. CT scan files are available on request.

Acknowledgements

We are grateful to Emmanuelle Fontoura Machado (Universidade Federal de Santa Maria - UFSM) for providing the CT scan files of *Axis* and to Roman Croitor for his help with literature on fossil deer endocasts. We also thank Bruno Esattore (Department of Ethology, Institute of Animal Science, Prague, Czech Republic), and Vlastimil Hart, and Jiří Turek (Department of Game Management and Wildlife Biology, Faculty of Forestry and Wood Sciences, Czech University of Life Sciences) for providing CT scan files of modern *Dama* and *Cervus elaphus*. We are grateful to Mauro Brilli (Istituto di Geologia Ambientale e Geoingegneria, Centro Nazionale delle Ricerche - IGAG-CNR) for technical collaboration for the isotopic analysis. We thank the "Azienda Sanitaria USL Toscana Centro" for granting access to their CT scanner facilities in the framework of an agreement between the "Fondazione Santa Maria Nuova Onlus" and the Earth Sciences Department of the University of Florence (responsible L.R.). The research was funded by the Spanish Ministry of Science, Innovation, and Universities ("Juan de la Cierva - Formación", ref. FJC2020-042982-I to F.S.), Regione Lazio ("Programma Fondo Sociale Europeo Plus - FSE+ 2021–2027, Codice SIGEM 22009D, ref. 22009DP000000516 to F.S.) and Sapienza University of Rome ("Bando di Ateneo - Avvio alla Ricerca 2017", ref. AR11715C7-CE78D4F to F.S.).

Appendix A. Supplementary data

Supplementary data to this article can be found online at https://doi.org/10.1016/j.quascirev.2024.108719.

References

Abbazzi, L., Benvenuti, M., Boschian, G., Dominici, S., Masini, F., Mezzabotta, C., Rook, L., Valleri, G., Torre, D., 1996. The Neogene and Pleistocene succession and the mammal faunal assemblages of an area between Apricena and poggio Imperiale (foggia). Memor. Soc. Geol. Ital. 51, 383–402.

Ackermans, N., 2020. The history of mesowear: a review. PeerJ 8, e8519.

Alcocks, J.P.H., 1988. Veld types of South Africa (An update of the first edition published in 1953). Mem. Bot. Surv. S. Afr. 57, 1–146.

Aguirre, E., De Andrés, I., 1974. Un molde endocraneano de *Praedama* (Cervido) del Pleistoceno Medio de Madrid. Quaternaria 18, 303–330.

Alekseeva, L.I., 1977. Theriofauna of eastern Europe early anthropogene. Transactions of the Geological Institute 300, 3–108 [in Russian].

Arzarello, M., Marcolini, F., Pavia, G., Pavia, M., Petronio, C., Petrucci, M., Rook, L., Sardella, R., 2007. Evidence of earliest human occupation in Europe: the site of Pirro Nord (southern Italy). Naturwissenschaften 94, 107–112.

Arzarello, M., Pavia, G., Peretto, C., Petronio, C., Sardella, R., 2012. Evidence of an early Pleistocene hominin presence at Pirro Nord (Apricena, foggia, southern Italy): P13 site. Quat. Int. 267, 56–61.

Arzarello, M., De Weyer, L., Peretto, C., 2016. The first European peopling and the Italian case: peculiarities and "opportunism.". Quat. Int. 393, 41–50.

Azzaroli, A., 1992. The cervid genus *Pseudodama* n.g. in the Villafranchian of Tuscany. Palaeontogr. Ital. 79, 1–41.

Azzaroli, A., 2001. On fossil deer from the valdarno, tuscany, Italy (comments on a paper by di Stefano & Petronio). Neues Jahrbuch Geol. Palaontol. Monatsh. 2001, 168–174.

Azzaroli, A., Mazza, P., 1992. The cervid genus *Eucladoceros* in the early Pleistocene of Tuscany. Palaeontogr. Ital. 79, 43–100.

Beccari, N., 1922. II getto lapideo della cavita endocranica di un Ungulato pliocenico della Valdelsa (Toscana). Monit. Zool. Ital. 33, 147–158.

Bedetti, C., Pavia, M., 2013. Early Pleistocene birds from Pirro Nord (puglia, southern Italy). Palaeontograph. Abteilung 298, 31–53.

Bellucci, L., Bona, F., Corrado, P., Magri, D., Mazzini, I., Parenti, F., Scardia, G., Sardella, R., 2014. Evidence of late gelasian dispersal of african fauna at Coste san Giacomo (anagni basin, central Italy): early Pleistocene environments and the background of early human occupation in Europe. Quat. Sci. Rev. 96, 72–85.
Berruti, G.L.F., Arzarello, M., 2016. Talking stones: taphonomy of the lithic assemblage of Pirro Nord 13 (Apricena, FG, Italy). A new approach to the study of the post depositional alterations on lithics tools. J. Archaeol. Sci.: Report 31, 102282.
Blain, H.A., Fagoaga, A., Ruiz-Sánchez, F.J., Bisbal-Chinesta, J.F., Delfino, M., 2019. Latest Villafranchian climate and landscape reconstructions at Pirro Nord (southern Italy). Geology 47, 829–832.
Bocherens, H., Koch, P.L., Mariotti, A., Geraads, D., Jaeger, J.-J., 1996. Isotopic biogeochemistry (^{13}C, ^{18}O) of mammal enamel from African Pleistocene hominid sites: implications for the preservation of paleoclimatic isotopic signals. Palaios 11, 306–318.
Bocherens, H., Jacques, L., Ogle, N., Moussa, I., Kalin, R., Vignaud, P., Brunet, M., 2009. Reply to the comment by A. Zazzo, W.P Patterson and T.C. Prokopiuk on "Implications of diagenesis for the isotopic analysis of Upper Miocene large mammalian herbivore tooth enamel from Chad" by Jacques et al. (2008). Palaeogeography, Palaeoclimatology, Palaeoecology 266. Palaeogeogr. Palaeoclimatol. Palaeoecol. 277, 200–210, 269–271.
Bocherens, H., 2014. Diet and ecology of the Scladina Neanderthal child: insights from stable isotopes. In: Toussaint, M. (Ed.), The Juvenile Neandertal Facial Remains from Scladina Cave, vol. 134, pp. 345–356. ERAUL.
Breda, M., Lister, A.M., 2013. *Dama roberti*, a new species of deer from the early Middle Pleistocene of Europe, and the origins of modern fallow deer. Quat. Sci. Rev. 69, 155–167.
Breda, M., Kahlke, R.D., Lister, A.M., 2020. New results on cervids from the early Pleistocene site of Untermassfeld. In: Kahlke, R.D. (Ed.), Das Pleistozän von Untermassfeld bei Meiningen (Thüringen), vol. 4. Monographien des Römisch-Germanisches Zentralmuseum 40, pp. 1197–1249.
Bryant, J.D., Froelich, P.N., 1995. A model of oxygen isotope fractionation in body water of large mammals. Geochem. Cosmochim. Acta 59, 4523–4537.
Cerling, T.E., Harris, J.M., 1999. Carbon isotope fractionation between diet and bioapatite in ungulate mammals and implications for ecological and paleoecological studies. Oecologia 120, 347–363.
Cherin, M., Breda, M., Esattore, B., Hart, V., Turek, J., Porciello, F., Angeli, G., Holpin, S., Iurino, D.A., 2022. A Pleistocene Fight Club revealed by the palaeobiological study of the *Dama*-like deer record from Pantalla (Italy). Sci. Rep. 12, 13898.
Cherin, M., Basilici, G., Duval, M., Shao, Q., Sier, M.J., Parès, J.M., Gliozzi, E., Mazzini, I., Magri, D., Di Rita, F., Iurino, D.A., Azzarà, B., Margaritelli, G., Pazzaglia, F., 2023. The dawn of the late villafranchian: paleoenvironment and age of the Pantalla paleontological site (Italy; early Pleistocene). Quat. Sci. Rev. 316, 108279.
Combourieu-Nebout, N., Bertini, A., Russo-Ermolli, E., Peyron, O., Klotz, S., Montade, V., Fauquette, S., Allen, J., Fusco, F., Goring, S., Huntley, B., Joannin, S., Lebreton, V., Magri, D., Martinetto, E., Orain, R., Sadori, L., 2015. Climate changes in the central Mediterranean and Italian vegetation dynamics since the Pliocene. Rev. Palaeobot. Palynol. 218, 127–147.
Croitor, R., 2006. Early Pleistocene small-sized deer of Europe. Hellenic Journal of Geosciences 41, 89–117.
Croitor, R., 2014. Deer from Late Miocene to Pleistocene of Western Palearctic: matching fossil record and molecular phylogeny data. Zitteliana B 32, 115–153.
Croitor, R., 2018. Plio-pleistocene deer of western palearctic: taxonomy, systematics. Phylogeny. Institute of Zoology of the Academy of Sciences of Moldova, p. 140.
Czyżewska, T., 1960. Nowy gatunek jelenia rodzaju Cervocerus Khomenko z plioceńskiej brekcji kostnej z Węzów. Acta Palaeontol. Pol. 5, 283–318 (In Polish, English summary).
Czyzewska, T., 1982. Natural endocranial casts of the Cervidae from Węże I near Dzialoszyn (Poland). Acta Zoologica Cracoviensia 26/1, 1–7.
D'Angela, D., Longinelli, A., 1990. Oxygen isotopes in living mammal's bone phosphate: further results. Chem. Geol.: Isotope Geoscience Sector 86, 75–82.
Dansgaard, W., 1964. Stable isotopes in precipitation. Tellus 16, 436–468.
De Giuli, C., Masini, F., Torre, D., 1987. The latest villafranchian faunas of Italy. The Pirro Nord local fauna (Gargano). Palaeontogr. Ital. 74, 52–62.
DeMiguel, D., Quiralte, V., Azanza, B., Montoya, P., Morales, J., 2012. Dietary behaviour and competition for vegetal resources in two Early Miocene pecoran ruminants from Central Spain. Geodiversitas 34, 425–443.
de Lumley, H., Kahlke, H.-D., Moigne, A.-M., Moullé, P.-E., 1988. Les faunes des grands Mammifères de la Grotte du Vallonnet Roquebrune-Cap-Martin, Alpes-Maritimes. L'Anthropologie 92, 465–496.
De Vos, J., Reumer, J.W.F., 1995. Early Pleistocene Cervidae (mammalia, artiodactyla) from the oosterschelde (The Netherlands), with a revision of the cervid genus *Eucladoceros* falconer, 1868. Deinsea 2, 95–121.
Di Stefano, G., Petronio, C., 1998. Origin of and relationships among the *Dama*-like cervids in Europe. Neues Jahrbuch Geol. Palaontol. Abhand. 207, 37–55.
Di Stefano, G., Petronio, C., 2002. Systematics and evolution of the eurasian plio-pleistocene tribe Cervini (artiodactyla, mammalia). Geol. Rom. 36, 311–334.
Duval, M., Arnold, L.J., Jean-Jacques, Bahain, Parés, J.M., Demuro, M., Christophe, Falguères, Shao, Q., Voinchet, P., Arnaud, J., Berto, C., Luigi, G., Daffara, S., Sala, B., Arzarello, M., 2024. Re-examining the earliest evidence of human presence in western Europe: new dating results from Pirro Nord (Italy). Quat. Geochronol. 101519–101519.
Fontoura, E., Ferreira, J.D., Bubadué, J., Ribeiro, A.M., Kerber, L., 2020. Virtual brain endocast of *Antifer* (Mammalia: Cervidae), an extinct large cervid from South America. J. Morphol. 281, 1223–1240.
Fortelius, M., Solounias, N., 2000. Functional characterization of ungulate molars using the abrasion-attrition wear gradient: a new method for reconstructing paleodiets. Am. Mus. Novit. 3301, 1–35.
Fortelius, M., Eronen, J., Liu, L., Pushkina, D., Tesakov, A., Vislobokova, I., Zhang, Z., 2006. Late Miocene and Pliocene large land mammals and climatic changes in Eurasia. Palaeogeogr. Palaeoclimatol. Palaeoecol. 238, 219–227.
Freudenthal, M., 1971. Neogene vertebrates from the Gargano Peninsula. Scripta Geol. 3, 1–10.
Gliozzi, E., Abbazzi, L., Azzaroli, A., Caloi, L., Capasso Barbaro, L., Di Stefano, G., Esu, D., Ficcarelli, G., Girotti, O., Kotsakis, T., Masini, F., Mazza, P., Mezzabotta, C., Palombo, M.R., Petronio, C., Rook, L., Sala, B., Sardella, R., Zanalda, E., Torre, D., 1997. Biochronology of selected mammals, molluscs and ostracods from the middle Pleistocene to the late Pleistocene in Italy. Riv. Ital. Paleontol. Stratigr. 90, 369–388.
Gordon, K.D., 1982. A study of microwear on chimpanzee molars: implications for dental microwear analysis. Am. J. Phys. Anthropol. 59, 195–215.
Grine, F.E., 1986. Dental evidence for dietary differences in *Australopithecus* and *Paranthropus*: a quantitative analysis of permanent molar microwear. J. Hum. Evol. 15, 783–822.
Grubb, P., 2005. Species *Axis axis*. In: Wilson, D.E., Reeder, D.M. (Eds.), Mammal Species of the World: A Taxonomic and Geographic Reference, third ed. Johns Hopkins University Press, p. 661.
Head, M.J., Gibbard, P.L., 2005. Early-Middle Pleistocene Transitions: an Overview and Recommendation for the Defining Boundary, vol. 247. Geological Society, London, Special Publications, pp. 1–18.
Head, M.J., Gibbard, P.L., 2015. Early–Middle Pleistocene transitions: linking terrestrial and marine realms. Quat. Int. 389, 7–46.
Hill, D., Bolton, K., Haywood, A., 2017. Modelled ocean changes at the Plio-Pleistocene transition driven by Antarctic ice advance. Nat. Commun. 8, 14376.
Kaiser, T.M., 2009. *Anchitherium aurelianense* (Equidae, Mammalia): a brachydont "dirty browser" in the community of herbivorous large mammals from Sandelzhausen (Miocene, Germany). Paläontol. Z. 83, 131–140.
Kaiser, T.M., Solounias, N., 2003. Extending the tooth mesowear method to extinct and extant equids. Geodiversitas 25, 321–345.
Kahlke, H.D., 1997. Die Cerviden- Reste aus dem Unter-pleistozän von Untermaßfeld. In: Kahlke, R.D. (Ed.), Das Pleistozän von Untermassfeld bei Meiningen (Thüringen), vol. 1. Monographien des Römisch-Germanisches Zentralmuseum, pp. 181–275, 40.
Kahlke, H.D., 2001. Neufunde von Cerviden-Resten aus dem Unterpleistozän von Untermassfeld. In: Kahlke, R.D. (Ed.), Das Pleistozän von Untermassfeld bei Meiningen (Thüringen), vol. 2. Monographien des Römisch-Germanisches Zentralmuseum 40, pp. 461–482.
King, T., Andrews, P., Boz, B., 1999. Effect of taphonomic processes on dental microwear. Am. J. Phys. Anthropol. 108, 359–373.
Koch, P.L., Hoppe, K.A., Webb, S.D., 1998. The isotopic ecology of late Pleistocene mammals in North America: Part 1. Florida. Chem. Geol. 152, 119–138.
Kohn, M.J., Cerling, T.E., 2002. Stable isotope compositions of biological apatite. Rev. Mineral. Geochem. 48, 455–488.
Lecuyer, C., Balter, V., Martineau, F., Fourel, F., Bernard, A., Amiot, R., Gardien, V., Otero, O., Legendre, S., Panczer, G., Simon, L., Martini, R., 2010. Oxygen isotope fractionation between apatite-bound carbonate and water determined from controlled experiments with synthetic apatites precipitated at 10–37 °C. Geochem. Cosmochim. Acta 74, 2072–2081.
Lisiecki, L.E., Raymo, M.E., 2005. A Pliocene-Pleistocene stack of 57 globally distributed benthic $\delta^{18}O$ records. Paleoceanography 20, 1–17.
Longinelli, A., 1984. Oxygen isotopes in mammal bone phosphate: a new tool for paleohydrological and paleoclimatological research? Geochem. Cosmochim. Acta 48, 385–390.
López-García, J.M., Luzi, E., Berto, C., Peretto, C., Arzarello, M., 2015. Chronological context of the first hominin occurrence in southern Europe: the *Allophaiomys ruffoi* (arvicolinae, rodentia, mammalia) from Pirro 13 (Pirro Nord, apulia, southwestern Italy). Quat. Sci. Rev. 107, 260–266.
Maul, L., Masini, F., Abbazzi, L., Turner, A., 1998. The use of different morphometric data for absolute age calibration of some South- and Middle European arvicolid populations. Palaeontogr. Ital. 85, 111–151.
Mihlbachler, M.C., Solounias, N., 2006. Coevolution of tooth crown height and diet in oreodonts (Merycoidodontidae, Artiodactyla) examined with phylogenetically independent contrasts. J. Mamm. Evol. 13, 11–36.
Mihlbachler, M.C., Beatty, B.L., Caldera-Siu, A., Chan, D., Lee, R., 2012. Error rates and observer bias in dental microwear analysis using light microscopy. Palaeontol. Electron. 15, 12–22.
Moe, S.R., Wegge, P., 1994. Spacing behaviour and habitat use of axis deer (*Axis axis*) in lowland Nepal. Can. J. Zool. 72, 1735–1744.
Muttoni, G., Giancarlo, Scardia, Kent, D.V., 2010. Human migration into Europe during the late Early Pleistocene climate transition. Palaeogeogr. Palaeoclimatol. Palaeoecol. 296, 79–93.
Muttoni, G., Giancarlo, Scardia, Kent, D.V., Enrico, Morsiani, Fabrizio, Tremolada, Cremaschi, M., Peretto, C., 2011. First dated human occupation of Italy at ~0.85 Ma during the late Early Pleistocene climate transition. Earth Planet Sci. Lett. 307, 241–252.
O'Leary, M.H., 1988. Carbon isotopes in photosynthesis. Bioscience 38, 328–336.
Pavia, M., Zunino, M., Coltorti, M., Angelone, C., Arzarello, M., Bagnus, C., Bellucci, L., Colombero, S., Marcolini, F., Peretto, C., Petronio, C., Petrucci, M., Pieruccini, P., Sardella, R., Tema, E., Villier, B., Pavia, G., 2012. Stratigraphical and palaeontological data from the early Pleistocene Pirro 10 site of Pirro Nord (puglia, south eastern Italy). Quat. Int. 267, 40–55.
Petronio, C., 1979. *Dama nestii eurygonos* Azz. di Capena (Roma). Geol. Rom. 18, 105–125.

Petronio, C., Krakhmalnaya, T., Bellucci, L., Di Stefano, G., 2007. Remarks on some Eurasian pliocervines: characteristics, evolution, and relationships with the tribe Cervini. Geobios 40, 113–130.
Petronio, C., Bellucci, L., Di Stefano, G., 2013. *Axis eurygonos* from Pirro Nord (Apricena, southern Italy). Palaeontograph. Abteilung 298, 169–181.
Pfeiffer, T., 1999. Die Stellung von Dama (Cervidae, Mammalia) im System plesiometacarpalerHirsche des Pleistozäns. Phylogenetische Rekonstruktion, metrische Analyse. Senckenbergische Naturforschende Gesellschaft 211, 1–218.
Rivals, F., Solounias, N., Mihlbachler, M.C., 2007. Evidence for geographic variation in the diets of late Pleistocene and early Holocene Bison in North America, and differences from the diets of recent plains Bison. Quaternary Research 68, 338–346.
Sardella, R., Bellucci, L., Bona, F., Cherin, M., Iurino, D.A., Rook, L., 2018. Before and after the earliest *Homo* dispersal in Europe: evidence from the early Pleistocene sites of the Italian Peninsula. Comptes Rendus Palevol 17, 287–295.
Semprebon, G.M., Rivals, F., 2007. Was grass more prevalent in the pronghorn past? An assessment of the dietary adaptations of Miocene to Recent Antilocapridae (Mammalia: artiodactyla). Palaeogeogr. Palaeoclimatol. Palaeoecol. 253, 332–347.
Skrzypek, G., Wisniewski, A., Grierson, P.F., 2011. How cold was it for Neanderthals moving to Central Europe during warm phases of the last glaciation? Quat. Sci. Rev. 30, 481–487.
Smith, B.N., Epstein, S., 1971. Two Categories of $^{13}C/^{12}C$ ratios for higher plants. Plant Physiology 47, 380–384.
Solounias, N., Semprebon, G., 2002. Advances in the reconstruction of ungulate ecomorphology with application to early fossil equids. Am. Mus. Novit. 3366, 1–49.
Strani, F., 2021. Impact of Early and Middle Pleistocene major climatic events on the palaeoecology of Southern European ungulates. Hist. Biol. 33, 2260–2275.
Strani, F., DeMiguel, D., Sardella, R., Bellucci, L., 2015. Paleoenvironments and climatic changes in the Italian Peninsula during the early Pleistocene: evidence from dental wear patterns of the ungulate community of Coste san Giacomo. Quat. Sci. Rev. 121, 28–35.
Strani, F., DeMiguel, D., Bellucci, L., Sardella, R., 2018a. Dietary response of early Pleistocene ungulate communities to the climate oscillations of the Gelasian/Calabrian transition in Central Italy. Palaeogeogr. Palaeoclimatol. Palaeoecol. 499, 102–111.
Strani, F., Profico, A., Manzi, G., Pushkina, D., Raia, P., Sardella, R., DeMiguel, D., 2018b. MicroWeaR: A new R package for dental microwear analysis. Ecol. Evol. 8, 7022–7030.
Strani, F., DeMiguel, D., Alba, D.M., Moyà-Solà, S., Bellucci, L., Sardella, R., Madurell-Malapeira, J., 2019. The effects of the "0.9 Ma event" on the Mediterranean ecosystems during the Early-Middle Pleistocene transition as revealed by dental wear patterns of fossil ungulates. Quat. Sci. Rev. 210, 80–89.
van der Made, J., 2015. The latest Early Pleistocene giant deer *Megalcoeros novocarthaginiensis* n. sp. and the fallow deer *Dama* cf. *vallonnetensis* from Cueva Victoria (Murcia, Spain). Mastia 11–13, 269–323.
van der Made, J., 2001. Les ongulés d'Atapuerca. Stratigraphie et biogéographie. L'Anthropologie 105, 95–113.
van der Made, J., Rosell, J., Blasco, R., 2017. Faunas from Atapuerca at the Early-Middle Pleistocene limit: the ungulates from level TD8 in the context of climatic change. Quat. Int. 433, 296–346.
van der Made, J., 2019. The dwarfed "giant deer" *Megaloceros matritensis* n.sp. from the Middle Pleistocene of Madrid - A descendant of *M. savini* and contemporary to *M. giganteus*. Quat. Int. 520, 110–139.
van der Made, J., Rodríguez-Alba, J.J., Martos, J.A., Gamarra, J., Rubio-Jara, S., Panera, J., Yravedra, J., 2023. The fallow deer *Dama celiae* sp. nov. with two-pointed antlers from the Middle Pleistocene of Madrid, a contemporary of humans with Acheulean technology. Archaeological and anthropological sciences 15, 41.
Vogel, J.C., Fuls, A., Ellis, R.P., 1978. The geographic distribution of kranz grasses in southern Africa. South Afr. J. Sci. 75, 209–215.
Williams, S.H., Kay, R.F., 2001. A comparative test of adaptive explanations for hypsodonty in ungulates and rodents. J. Mamm. Evol. 8, 207–229.
Zunino, M., Pavia, M., Fernández-López, S.R., Pavia, G., 2012. Taphonomic analysis of the lower Pleistocene Pirro Nord fossil locality (Pirro 10 site, Puglia, southern Italy): a depositional model for vertebrate assemblages in a karstic environment. Palaios 27, 3–18.